Mid-to Late Holocene landscape reconstruction of the Maye Estuary (Picardy, Northern France) and its implications for human occupation

Stéphane Desruelles, Matthieu Ghilardi, Christophe Cloquier, Doriane Delanghe, Yannick Buchot, Daniel Hermitte, Jean-Claude Parisot, Jean-Marc Hoeblich

Quaternary International

Mid- to Late Holocene landscape reconstruction of the Maye Estuary (Picardy, Northern France) and its implications for human occupation

--Manuscript Draft--

Manuscript Number:	QUATINT-D-19-00169R1
Article Type:	Full Length Article
Keywords:	geoarchaeology; palaeogeography; Sedimentology; Relative sea level rise; Coastal plain; Holocene
Corresponding Author:	Stéphane Desruelles University Paris-Sorbonne Paris, FRANCE
First Author:	Stéphane Desruelles, Dr
Order of Authors:	Stéphane Desruelles, Dr
	Matthieu GHILARDI
	Christophe CLOQUIER
	Doriane DELANGHE
	Yannick BUCHOT
	Daniel HERMITTE
	Jean-Claude PARISOT
	Jean-Marc HOEBLICH
Abstract:	The town of Rue was one of the most important coastal harbours of Picardy, Northern France, from the beginning of the 12 th century to the end of the 15th century CE. Document sources and ancient maps confirm the existence of this vibrant harbour. Until now, however, no palaeoenvironmental studies have attempted to reconstruct the configuration of the region's coastline during medieval times. Here we employ a geoarchaeological approach to reconstruct the Mid- to Late Holocene shoreline and landscape changes in the Rue area. Our approach includes a geophysical survey (Electric Resistivity Tomography method) and a series of eight sediment cores that reveal the region's chronostratigraphy. Document sources were also used to shed light on the landscape configuration during the Late Middle Ages (ca. 1300 CE). Our coring results, based on sedimentological analyses, are combined with 2D geophysical profiles down to 21.50 m. This reveals, firstly, that a calm marine environment prevailed at the beginning of the 4th millennium BCE, particularly in depressions bordered by Pleistocene coastal spits (foraines). Secondly, from ca. 3500 BCE to ca. 1000 BCE, coastal swamps predominated. Then, thirdly, at around 1000–1250 CE, an estuarine depositional environment prevailed, prior to a final period of land reclamation of the former Maye Estuary from the 13th century CE onwards. These results agree well with recent work on sea level changes along the Atlantic and English Channel coasts of France, where continuous post-glacial sea level rise has been observed. Our study also proposes a location of the medieval harbour of Rue to the west of the town at the upstream boundary of the upper part of the Maye Estuary, near ' Le Moulin de Saint-Jean' , although archaeological evidence of the exact site of this tidal harbour is still lacking.
Suggested Reviewers:	Alain Trentesaux, Dr Pr, Universite de Lille Faculte des Sciences et Technologies alain.trentesaux@univ-lille.fr
	Pierre Stephan, Dr Littoral environnement teledetection et geomatique pierre.stephan@univ-brest.fr
	Sylvie Coutard, Dr INRAP: Institut national de recherches archeologiques preventives sylvie.coutard@inrap.fr

Response to Reviewers:	

15/12/2019

Thijs van Kolfschoten
Editor in Chief
Quaternary International

Dear Editor:

I wish to submit a research paper for publication in Quaternary International titled 'Geoarchaeology of the Maye estuary (Picardy, Northern France): Mid- to Late Holocene landscape reconstruction and its implications for human occupation'. The paper was coauthored by Matthieu Ghilardi, Christophe Cloquier, Doriane Delanghe, Yannick Buchot, Daniel Hermitte, Jean-Claude Parisot, and Jean-Marc Hoeblich.

This study reconstructs the geoarchaeology of the Maye estuary in Northern France, combining geophysical and chronostratigraphical investigations with the analysis of historical sources. We provide a detailed description of the palaeoenvironment during the last 5000 years and make inferences about human settlement and land reclamation in the area. We believe that our study makes a significant contribution to the literature because a detailed palaeoenvironmental investigation of the Maye estuary has not been performed before, and our study additionally provides new information about the probable position of the medieval harbour of the town of Rue, the precise location of which was unknown.

We believe that this paper will be of interest to the readership of your journal due to its broad audience of scientists dealing with physical and natural issues in the Quaternary.

Please consider, as potential referees, Pr. Dr. Alain Trentesaux (Faculté des Sciences et Technologies, Université de Lille; alain.trentesaux@univ-lillefr) and Dr. Pierre Stéphan (UMR6554 LETG, CNRS; pierre.stephan@univ-brest.fr).

This manuscript has not been published or presented elsewhere in part or in entirety and is not under consideration by another journal. We have read and understood your journal's policies, and we believe that neither the manuscript nor the study violates any of these. There are no conflicts of interest to declare.

Thank you for your consideration. I look forward to hearing from you.

Sincerely,
Dr. Stéphane Desruelles
UFR de Géographie et Aménagement, FRE 2026 ENeC, Faculté des Lettres, Sorbonne Université, CNRS
191 rue Saint-Jacques, 75005 Paris, France
+33663068802
stephanedesruelles@gmail.com

Mid- to Late Holocene landscape reconstruction of the Maye Estuary (Picardy, Northern France) and its implications for human occupation

Stéphane DESRUELLES[a*], Matthieu GHILARDI[b], Christophe CLOQUIER[c], Doriane DELANGHE[b], Yannick BUCHOT[b], Daniel HERMITTE[b], Jean-Claude PARISOT[b], Jean-Marc HOEBLICH[d]

[a] UR Médiations - Sciences des lieux, sciences des liens, Faculté des Lettres, Sorbonne Université

[b] UMR 7330 CEREGE, Aix-Marseille University, CNRS, IRD, Collège de France, INRAE. Europôle de l'Arbois BP 80, 13545 Aix-en-Provence CEDEX 04, France.

[c] UMR 8589 LaMOP, Université de Paris 1 Panthéon-Sorbonne - CNRS

[d] UFR d'histoire-géographie, Université de Picardie Jules-Verne, Amiens

*corresponding author

Email: stephanedesruelles@gmail.com Phone: +33663068802

Abstract

The town of Rue was one of the most important coastal harbours of Picardy, Northern France, from the beginning of the 12th century to the end of the 15th century CE. Document sources and ancient maps confirm the existence of this vibrant harbour. Until now, however, no palaeoenvironmental studies have attempted to reconstruct the configuration of the region's coastline during medieval times. Here we employ a geoarchaeological approach to reconstruct the Mid- to Late Holocene shoreline and landscape changes in the Rue area. Our approach includes a geophysical survey (Electric Resistivity Tomography method) and a series of eight sediment cores that reveal the region's chronostratigraphy. Document sources were also used to shed light on the landscape configuration during the Late Middle Ages (ca. 1300 CE). Our coring results, based on sedimentological analyses, are combined with 2D geophysical profiles down to 21.50 m. This reveals, firstly, that a calm marine environment prevailed at the beginning of the 4th millennium BCE, particularly in depressions bordered by Pleistocene coastal spits (*foraines*). Secondly, from *ca.* 3500 BCE to *ca.* 1000 BCE, coastal swamps predominated. Then, thirdly, at around 1000–1250 CE, an estuarine depositional environment prevailed, prior to a final period of land reclamation of the former Maye Estuary from the 13th

century CE onwards. These results agree well with recent work on sea level changes along the Atlantic and English Channel coasts of France, where continuous post-glacial sea level rise has been observed. Our study also proposes a location of the medieval harbour of Rue to the west of the town at the upstream boundary of the upper part of the Maye Estuary, near '*Le Moulin de Saint-Jean'*, although archaeological evidence of the exact site of this tidal harbour is still lacking.

Keywords:
Geoarchaeology; Palaeogeography; Sedimentology; Relative sea level rise; Coastal plain; Holocene

1. Introduction

Over the last decades, particular attention has been paid to the study of palaeoenvironmental dynamics combined with the human settlement of the French coastal plains of Brittany, Normandy, and Picardy (Lespez et al., 2004; Gandouin, 2007; Lespez et al., 2010; Pailler et al., 2011; Stéphan, 2011; Lequint and Fouache, 2012; Daire et al., 2013). However, the Bay of Somme has been little investigated from a geoarchaeological perspective, despite its long term history of human activity.

The town of Rue is located on the Picardy coastal plain, approximately 7 km from the present-day coastline (Fig. 1). It was one of the most important coastal harbours of Picardy during medieval times, from the beginning of the 12th century to the end of the 15th century CE (Labrecque, 2008). It is generally accepted that this harbour gradually silted up due to a natural infilling of the estuary with sediment, reinforced by structures (artificial levees in particular) built for agricultural land reclamation purposes on the coastal plain from the 12th century CE (e.g., Demangeon, 1905). However, no prior palaeoenvironmental or geomorphological studies have involved the scrutiny of ancient sketches, maps and plans in the endevour to reconstruct shoreline displacements during medieval times.

This paper aims to reconstruct the landscape evolution surrounding the medieval town of Rue and discusses relative sea level change and related morphological impacts on the evolution of the former Maye Estuary over the last 5000 years.

2. Physical setting and historical context

2.1. Topographic, geological, and tectonic settings

The town of Rue is situated in the south of the Picardy coastal plain, which extends between the Bay of Somme to the south-west and Authie Bay to the north. This flat land is characterized by an average height of about +4.50 m above mean sea level (a.m.s.l.). It developed to the west of a relict cliff bordering a plateau composed of Upper Cretaceous chalk with flint (BRGM, 1981) and was built up primarily from wet or drained lowlands (Demangeon, 1905; Munaut and Gilot, 1977; Le Fournier, 1974, 1980) which surrounded relict Pleistocene coastal spits composed of rounded pebbles and blocks (called 'Formation de Rue'; Agache et al., 1963; Ters et al., 1980; BRGM, 1981; Fig. 1). These spits (locally called '*foraines'*) tend to form in a north/south direction and have a maximum elevation of between +9 and +13 m a.m.s.l. The medieval town of Rue is located at about +7 m a.m.s.l. and is built on the Rue *foraine,* which was locally incised by small river channels and filled with Holocene marine and continental sediments (Ters et al., 1980). The coastal plain is bordered to the west by a coastal dune ridge rising to +36 m NGF which has established over the last 5500 years (Le Fournier, 1974, 1980; Meurisse, 2005; Meurisse-Fort, 2007).

According to BRGM (1981), the relict cliff probably formed through faulting (Fig. 1). In addition, the coastal plain was likely divided into pieces by a system of faults and flexures whose movements contributed to the sedimentary filling in of the former undated 'Gulf of Rue'. BRGM (1981) estimates that these movements have caused the Rue area to uplift by about 5 m since the 18th century CE. According to Goffé et al. (1998), an active northwest-southeast strike-slip fault north of the Bay of Somme may have raised the northern compartment, corresponding to the Rue area. A series of earthquakes occurred during medieval times, for example in 1467 CE, when such an event damaged the church of Saint-Wulphy (Labrecque, 2008), and in 1580 CE when another earthquake affected the town of Abbeville (Louandre, 1844-1845).

Conditions along the coastline are megatidal with tidal range varying from 5 m to 8.65 m at Cayeux-sur-Mer, in the south of the Bay of Somme (SHOM, 2017). The mean high-water springs (MHWS) are situated at +5.41 m NGF (4.36 m a.m.s.l.) and the level of the highest astronomical (extreme) tide is +6.13 m NGF (5.09 m a.m.s.l.). Highest sea level can reach approximately +6.45 m a.m.s.l. with a 100-year return period (SOGREAH, 1995). According to Goslin (2014), the tidal range has undergone only slight changes since 6000 BCE (a maximum 0.70 m increase) in Brittany (western France). The coastal plain is exposed to storm-

surge flooding caused by dune breaching. The prevailing wind is in the west-southwest direction and the longshore drift moves sediments northward (Bastide, 2011; Michel, 2016). South of the study area, the Bay of Somme is a hyper-tidal (Trenteseaux et al., 2012) and mixed estuary (Dalrymple et al., 1992;) which has filled in with marine sands (BRGM, 1981, 1985; Michel, 2016).

2.2. Holocene sea level changes and coastal evolution in north-western Europe

Holocene sea level changes and related coastal evolution are generally considered to be influenced by the interplay between several factors (e.g. Goslin et al., 2013): (1) eustatism, (2) isostatic processes (Vink et al., 2007; Shennan et al., 2018), (3) tectonic activity, (4) local effects controlling the sedimentary record, particularly sediment compaction (the effect of post-depositional consolidation; Long et al., 2006; Horton and Shennan, 2009; Marion et al., 2009; Brain et al., 2011) and changes in tidal regime, and (5), other unspecified, random, and hard-to-quantify factors which influence relative sea level reconstruction, particularly erosion of sedimentary sequences (Goslin et al., 2013). According to several recent papers, local factors (4 and 5) play a key role in the effect of sea level change on coastal system morphologies (Bungenstock and Weerts, 2010; Baeteman et al., 2011). The general geomorphological evolution of the north-western European coastal plains can be regarded as the cross combination of natural forcings (such as sea level change, variations in sediment supply and sediment distribution; e.g., Costa and Suanez, 2013; Pierik et al., 2017) and, for roughly the last 2000 years, a mixture of natural and anthropogenic factors (Pierik et al., 2017).

Previous research conducted in the southern Picardy coastal plain did not attempt to precisely reconstruct the geomorphological evolution of the Rue area, despite sediment cores being drilled in the vicinity of Rue in the 1980s (Lefèvre et al., 1980; Ters et al., 1980; Figs. 1 and 3). However, the goal of those studies was not the reconstruction of the former shoreline position west of the town so as to locate its medieval coastal harbour. The published ^{14}C dating results were recalibrated by Meurisse-Fort (2007) using the IntCal13 calibration curve (Reimer et al., 2013). In addition, Meurisse-Fort (2007) considered the influence of sediment hydrocompaction on her chronostratigraphies to reconstruct the Holocene sea level evolution. However, the role of sediment hydrocompaction remains difficult to quantify (e.g., Allen, 2000; Goslin et al., 2013; Brain, 2015; Stéphan and Goslin, 2016; Shennan et al., 2018).

Along the Atlantic and English Channel coasts of France, some Holocene marine transgressions and regressions were identified by Ters (1973, 1986). Many papers have since adopted this description of Holocene transgression-regression cycles. For example, Meurisse-Fort (2007) reconstructed the coastline evolution of the Picardy coastal plain over the last 6000 years (see the red curve in Fig. 2):

- Around 4000 BCE, the sea level maximum was +2 m/+3 m a.m.s.l. with storm surges at *ca.* +6 m a.m.s.l.. The sea reached the foot of the present relict cliff. According to the stratigraphies published by Lefèvre et al. (1980) and Ters et al. (1980) and recalibrated by Meurisse-Fort (2007; date recalibration and consideration of sediment compaction), silts were deposited at the extreme limit of high waters at *ca.* + 3 m a.m.s.l. in the area of core Rue 3 (*ca*. 1.5 km west of the present town; Fig. 1).
- A marine regression occurred between *ca.* 4000 and 3100 BCE, with an increase in rainfall, peatland growth and development of coastal swamps. According to Meurisse-Fort (2007), the relative mean sea level was *ca.* −10 m a.m.s.l. at around 3100 BCE.
- A second marine transgression occurred from *ca.* 3100 BCE to 1400 BCE, during which shoreline impact varied greatly due to local geomorphological features. At the end of this phase, mean sea level was *ca.* −2 m/−3 m a.m.s.l.. Finally, around 2500–2000 BCE, the coastal plain was wider than it is today and consisted of a vast floodplain between bays and estuaries.
- From *ca.* 1400 BCE onward, the influence of aeolian dynamics and climate change exceeded the marine forcings. Mean sea level revealed few deviations from its present-day height. Storm-surge flooding caused by coastal barrier breaching played a greater role in landscape evolution, particularly between 450 BCE and 600–700 CE. However, shoreline stabilisation facilitated multi-stage processes of dune accretion.

  Around 1000 BCE, a peatland lay southwest of Rue, behind a sandbar (according to a dating published by Ters et al., 1980 and recalibrated by Meurisse-Fort, 2007). A more recent (831–1264 CE) freshwater peatland (according to a dating published by Lefèvre et al. (1980) and recalibrated by Meurisse-Fort (2007)), was identified southeast of Rue in core M21 (Fig. 1).

This outline of Holocene transgression-regression cycles is strongly challenged by recent works which take into account that for the last 10 kyr, there have been only small-scale fluctuations of global sea level in tectonically stable areas (e.g. Stéphan and Goslin, 2016). Along the

Atlantic and English Channel coasts of France, relative sea level is thought to have risen continuously during the last 8000 years, with a major deceleration of sea level rise around 4000 BCE (e.g. Mrani-Alaoui and Anthony, 2011; Goslin et al., 2013; Goslin, 2014; Stéphan et Goslin, 2016; Garcia-Artola et al., 2018; Fig. 2). The glacial isostatic component played a major role in increasing the rate of sea level rise between 4000 and 2000 BCE (Garcia-Artola et al., 2018). During the last 4000 years, according to the data published by Shennan and Horton (2002) for south-west England, relative sea level rise due to glacial isostatic adjustment was around 0.4 mm yr-1. Regarding the eustatic component, model ICE-5G (VM2a) published by Peltier (2004) indicates a relative sea level rise of approximately 1.1 mm yr-1 over the last 4000 years in our study area (Fig. 1).

While recent papers agree that relative sea level has continued to increase, they attribute to climate change the main effect on the geomorphological evolution of the coast of north-western Europe during the last 3500 years. Increased storminess and pluviometry were recorded at around 1000 BCE in north-western Europe (Gandouin, 2003; Dark, 2006; Clark and Rendell, 2009; Sorrel et al., 2012; Van Vliet-Lanoë et al., 2014a, 2014b; Pierik et al., 2017). Major changes in coastal sedimentary systems have been observed for this period along the coasts of both the English Channel (Long and Hughes, 1995; Lespez et al., 2010; Tessier et al., 2012) and the Atlantic (Pontee et al., 1998; Tastet and Pontee, 1998; Clave et al., 2001; Moura et al., 2007).

Pouzet et al. (2018) distinguish four main 'European Atlantic storm events' (EASEs) over the last 3500 years: 1300–1600 CE (EASE 1), 200–800 CE (EASE 2), 900–400 BCE (EASE 3) and 1500–1300 BCE (EASE 4). During these events, marine deposits may have been eroded by drainage network incision, increased river discharge may have favoured continental sediment supply, and coastal breaching may have caused river courses to shift (Goslin, 2014).

For the last 1000 years, the geomorphological evolution of the Picardy coastal plain has been strongly influenced by human activities and land reclamation for dike construction (Demangeon, 1905; Dobroniak, 2000). The first dike was likely built in the 12th century CE between '*Le Muret*' and '*La Petite Retz*' (Briquet, 1930), approximately 7 km north-northwest of Rue (Fig. 1). Dikes continued to be built until the 1860s (Briquet, 1930) north of the coastal plain, linked with the shifting of Authie Bay. In the south of the coastal plain, the former mouth of the Maye ('*Val de Maye*'; Fig. 1) is protected from coastal flooding by a dike built in 1835. However, storm-surge flooding still occurred (Meurisse-Fort, 2007), probably linked with

episodes of increased storminess which took place in north-western Europe from 100–950 CE and from1300–1700 CE (Sorrel et al., 2012; Pierik et al., 2017). Lefèvre et al. (1980) report marine flooding deposits in the area of core M21 (Fig. 1); these deposits covered the upper peat layer (Fig. 3) and may have occurred around 1300 CE.

2.3. Rue: a major harbour in the northwest of France from the beginning of the 12th century to the end of the 15th century CE

The Rue *foraine*, like all the Pleistocene bars of the Picardy coastal plain (Rougier, 2012), was favourable for human settlement at least from the Bronze Age (Rougier et al., 2008; Gapenne et al., 2017). An Early Bronze Age cemetery (Baray, 2001) and a rural peopling dating from the Iron Age (2nd–1st century BCE; Rougier and Blancquaert, 2001) were discovered together at the top of a Pleistocene bar, at a location called '*Le Chemin des Morts*', northeast of Rue. A coin hoard dated to the 3rd century CE (Ben Redjeb and Foucray, 1989) and the archaeological remains of a Gallo-Roman villa were discovered in the Bleue *foraine* (at *ca.* +9 m a.m.s.l.) south of Rue (Notte, 2002). Other remains have been unearthed at the top of Pleistocene bars (the Hère *foraine*; Rougier, 2012), indicating a human occupation since the Bronze Age, even the Neolithic (Gapenne et al., 2017).

Data also lack for the Early Middle Ages. It is generally accepted that the town flourished in the 12th century CE (Labrecque, 2008). This development can be attributed to a legend claiming that in 1101, a local villager of Rue discovered a boat washed up on the shore, in which was found a large wooden cross originating in Jerusalem. The wealth of the city was thereafter built on pilgrimages and trade (transport of goods by sea). As early as the 13th century, the harbour of Rue, which is thought to have been located in the Maye Estuary, was as important as those of the Bay of Somme (Delaporte, 1925). A municipal charter, recognised in 1210 by the Count of Ponthieu, testifies to the importance and diversity of production and trade (e.g. fishing, agriculture, farming, textiles; Labrecque, 2008). This suggests that the Count imposed high taxes on each ship entering the harbour.

At the end of the 13th century, a canal project to re-establish access to the sea was proposed to the inhabitants, which implies that the harbour had silted up. That project was never begun, but in 1277, a canal was dug to bring the Authie's flow towards the harbour, probably because of the increase in siltation (Labrecque, 2008). However, the westward shift of the shoreline seems to have gradually prevented access to the harbour by heavily laden ships arriving from the

Authie. Thus, harbour activity strongly decreased as early as the 14th century CE, even if commercial maritime activity continued during the 15th century CE (Labrecque, 2008).

Literary sources indicate that the town of Rue was naturally protected by the Maye to the north and west, and by marshes to the south and east (Delaporte, 1925). Following the Charter of 1210, fortification works (protecting walls) were built. These essentially took the form of ditches, on the edges of which stone houses and walls were built. The ramparts were likely widened in the 15th century before being pierced by five gates, with '*la porte de la grève*' (the shore gate) to the west (Poiret, 1931). The fortifications were destroyed in 1670, under the reign of Louis XIV, by order of Jean-Baptiste Colbert, Secretary of State of the Navy. The earliest map of Rue found in historical archives dates from 1640. A previous excavation near '*le bastion de Saint-Jean*' (Flucher, 2004) identified an embankment under the ravelin. This embankment diverted the course of the Maye. However, artefacts (mainly ceramics) discovered there provide only an imprecise chronology of the fortification works.

Present day landscape configuration does not enable to significantly demonstrate that Rue was a coastal town. Moreover, archaeological evidence is scarce, and the few historical sources fail to provide a robust and indisputable reconstruction of landscape evolution surrounding the medieval town of Rue. In an attempt to do so, we have conducted a palaeoenvironmental study.

3. Material and methods

Field investigations (geophysical survey and coring) were carried out northwest of Rue, particularly around '*la porte de la grève*', where the medieval port is thought to have been located in the upper part of the Maye Estuary. Field investigations were completed by laboratory analyses (sedimentological analysis and radiocarbon dating of drill core samples) and by the study of historical sources. All these data, as well as altimetry data 'RGE 1 m' provided by the 'Institut Géographique National', were integrated into a Geographic Information System database.

3.1. Electric resistivity tomography (ERT)

To evaluate both the geometry and thickness of surficial deposits and bedrock depth, and to locate archaeological structures, eight electrical resistivity tomography (ERT) profiles were established around the town of Rue (Figs. 4, 5a, 5b, and 5c).

ERT has been successfully used in various subsurface field studies, especially in geomorphology (Beauvais et al., 2007; Ghilardi et al., 2017) and archaeology (Siart et al., 2010; Quesnel et al., 2011; Ghilardi et al., 2015). The 2D subsurface profiles were obtained using the ABEM Lund Imaging System (Terrameter LS/4 channel) with an array of 64 electrodes with a Schlumberger-Wenner reciprocal layout protocol. A computer inversion program (Res2Dinv; Loke, 2003) that includes topography and generates images of the resistivity distribution was used.

To satisfactorily obtain data on the thickness of the surficial deposits and their organisation (Ritz et al., 1999), ERT profiles were conducted with an electrode distance ranging from 0.60 m (ERT6, with a maximum depth of 5.17 m) to 2.50 m (ERT3, with a maximum depth of 21.50 m).

Because different materials can have similar electrical properties, the ERT method does not allow for unequivocal interpretation. Therefore, two reference profiles were established on sites where the stratigraphy and/or lithology can be readily seen: ERT7, on an extraction site of Pleistocene gravels and pebbles, and ERT8, on a chalk plateau near Rue.

3.2. Sedimentological coring

Vibracores with a diameter of 50 mm were drilled to a maximum depth of 8.40 m below the surface (Fig. 4; Table 1) in May 2012 northwest of Rue using a Cobra TT vibrocorer with hydraulic extractor (Figs. 6 and 7). The position of the cores was chosen in accordance with the results obtained from the geophysical survey. Each core was precisely levelled using a theodolite and local IGN geodetic benchmarks were used as references.

3.3. Sedimentological analyses

The grain-size distribution of the fine fraction (<2 mm) was measured by laser diffraction granulometry at CEREGE. Preparation of the samples was based on Ghilardi et al. (2014). The grain-size distribution was then measured using a *Beckman Coulter LS 13 320* laser granulometer with a range of 0.04 to 2000 µm.

Loss-on-ignition (LOI) measurements were made at CEREGE, following Dean (1974), and Bengtsson and Enell (1986). Sediment samples of approximately 1 g were taken at 5 cm intervals throughout the core. After drying at 105 °C to a constant weight, the samples were heated to 550 °C for 7 h to estimate their organic matter content. A second heating phase, to 925 °C for a further 7 h, was undertaken to assess the proportion of carbonates.

Mollusc identification was conducted on all cores, but analyses were limited due to the paucity of these samples along the cores, and to the small sizes of thematerials which were retrieved.

3.4. AMS ^{14}C dating method

The chronostratigraphy of the cores was analysed at CEREGE using a series of 14 AMS radiocarbon determinations derived from charcoal, plant remains, wood samples and peat samples collected from the cores (Table 2). These analyses were performed at the Poznan Radiocarbon Dating Laboratory (Poland). Subsequent calibration of ^{14}C ages was conducted using the Calib Software Version 7.1 (Stuiver and Reimer, 1993) and the IntCal13 calibration curve (Reimer et al., 2013).

3.5. Examination of historical sources

Document sources provide diverse information on coastal landscapes, including physical environment (e.g. nature of the foreshore), constructions, and various human activities such as fish species caught, quantities of fish due for rent, goods transported by boats, places of loading and unloading, peat extraction, and relationships between coastline users and the authorities exercising rights.

For the study area, document sources regarding the medieval coastal landscapes are scarce, but those available are relatively varied and rich in information. Originally produced by municipalities or fiefdoms, they are today stored in various collections and series of the National Archives (Paris), the Departmental Archives of the Somme (Amiens), the National Library of France (BnF, Paris), and the Abbeville Municipal Library. A large part of the archives has unfortunately succumbed to the destruction provoked by successive wars. For example, the documents of the old series of the Abbeville Municipal Archives were lost as recently as 1940.

We implemented a regressive method to study the document sources, beginning with the analysis of the most recent documents. Unfortunately, for the study area, documentary sources

prior to the 13th century are relatively rare and provide no historical maps or figures until the early 16th century.

4. Results

4.1. Borehole chronostratigraphy

Pleistocene gravels, including rounded flint pebbles and marine shells in a matrix of fine sand (Ters et al., 1980), were found in the lowermost part of all cores situated west of Rue with a top bed depth that varied between 2 m and 7 m (Figs. 6, 7 and 8). This reveals the lateral heterogeneity and extension of these units. These formations were also identified in various ERT profiles (see § 4.2).

Above this first layer, four main morphosedimentary units were distinguished in cores R1, R2, R4, R5, R6, and R7 (Figs. 6, 7 and 8):

- Unit A (recorded in R4, R5, R6 and R7) contains medium grey silty sands. It can be divided into two subunits: from the base layer (-1.15m in R5) to *ca.* +0.70 m a.m.s.l., Subunit A1 comprises medium to fine sand (mean grain-size of *ca.* 210 µm and modal index of *ca.* 230 µm) and Subunit A2, from *ca* +0.70 m a.m.s.l., is composed of very fine to silty sand (mean of *ca.* 70 µm; modal index of *ca.* 65 µm and *ca*. 60% of particles <62 µm). This unit has a low carbonate content (less than 2.5%) and a significant number of macrocharcoals and plant debris are observed. The thickness (up to 2.50 m in R5) and the surface of this unit are irregular (between +0.90 m a.m.s.l. in R6 and +2.50 m a.m.s.l. in R2). The uppermost part of Unit A dates roughly from the beginning of the 4th millennium BCE (4057–3953 cal. BCE in R4, 3824–3695 cal. BCE in R5 (Figs. 6, 7 and 8).
  Because of the texture, colour, and chronology of the sediments in this unit, we determine that they were deposited by the sea, in a calm environment, particularly in depressions bordered by Pleistocene coastal spits (‘*foraines*’).

- Unit B (recorded in R4, R5, R6 and R7) consists of a peat accumulation rich in plant remains and exhibiting low $CaCO_3$ content (less than 5%). Large pieces of charcoal are visible but molluscs are absent. The height of the base of this formation varies according to the geometry of the underlying marine deposits, while the top of the unit is almost flat,

at about +2.60 to +2.90 m a.m.s.l. Generally, this unit dates from the early 4th to the late 2nd millennium BCE (3824–3695 cal. BCE in R6 and 1134–1004 cal. BCE in R7).

The characteristics of Unit B differ from core to core. R4 and R7 are homogeneous and rich in organic matter (around 60%). Between +1.25 m a.m.s.l. and +1.50 m a.m.s.l., R5 reveals a sandy layer between the peat accumulations. In R6, above +1.90 m a.m.s.l., relatively young (834–752 cal. BCE) dark grey peaty silts were identified.

The combined sedimentological and geochemical proxies described above lead us to conclude that this unit provides evidence of coastal swamp environments with sizable peat accumulation.

- Unit C, identified in cores R1, R2, R4, R5, R6 and R7, between about +2.60 m a.m.s.l. and +5.20 m a.m.s.l., from the 11th century to the beginning of the 13th century (989–1052 cal. CE and 1039–1210 cal. CE in R4), is not homogeneous from core to core.

  Up to about +4 m a.m.s.l., the unit mainly comprises very fine to silty sands (mean at *ca.* 75 µm and mode at *ca.* 65 µm) in almost all cores (R1, R2, R4, R5, R6, and R7). However, the clayey-silty fraction (<63 µm) was generally higher in the deposits found in R4 - and to a lesser extent in R7 - than that identified in R5 and R6. This difference indicates that the deposits occurred in calmer water in the areas from which R4 and R7 were taken. Between about +2.70 m and +3.20 m a.m.s.l., R5 and R6 show an intercalation of thin sandy layers with thin clayey beds that correspond to tidal rhythmites (Fig. 9). Such features were observed by Meurisse-Fort (2007) in the muddy saltmarsh areas of the Canche Estuary (located north of the Picardy coastal plain).

  In the uppermost part of Unit C (above +4 m a.m.s.l.), the stratigraphy differs from core to core:

  - Up to +5.20 m a.m.s.l., R4 consists of very fine oxidised sands (mean at ca. 67 µm and mode at ca. 76 µm), including marine to brackish bivalve fragments (*Cerastoderma edule*) typical of a sandy or muddy sand area of an estuary and enclosed bay (Bellamy et al., 2009), and charcoals dated to 989–1210 cal. CE. R1 and R2 contain coarser sediments (fine to medium sand; mean at ca. 250 µm and mode at ca. 260 µm) than that recorded in R4, R5, R6, and R7. Based on sedimentological and faunal (cockles) evidence, we surmise that these sediments (Subunit C1) were deposited in a marine environment.
  - Subunit C2, identified in R1, R2, R5, R6, and R7, contains fine material (very fine sands or silty sands; mean at *ca.* 122 µm and mode at *ca.* 75 µm). It exhibits a relatively higher

calcium carbonate content (>35%) in R1, R2, and R7. Between +4.40 m and +4.90 m a.m.s.l., the very fine sands recorded in R7 contain unidentifiable land snail debris. In R1, R2, and R5, this fine material is covered by a peat layer containing plant debris, dated to 380–536 cal. CE (in R5). We surmise that Subunit C2 were deposited in a riverine or swamp environment.

- In R6, we found a layer of fine sands between +4.40 m and +5.10 m a.m.s.l., characterised by a multimodal particle size distribution with secondary medium to coarse sand modes situated at 250 µm and 1000 µm. Even if they contain orange-coloured archaeological remains; it is difficult to determine which anthropogenic influence prevailed on these deposits (Subunit C3), and whether they are of marine or continental origin.

Unit C includes coarser sand beds that may correspond to lag deposits, recorded in R4 and R6 at *ca*. +4.30 m a.m.s.l. In R4, the bed is 0.05 m thick and is characterised by D_{90} at 805 µm. In R6, this layer is thicker (0.20 m) and is covered by finer marine deposits (Subunit C1) above a clear contact (erosional surface). These finer deposits are characterised by a D90 ranging from 403 to 660 µm. This bed is covered by fluvial deposits (Subunit C2), with a bottom layer that is relatively rich in CaCO3.

Coastal processes of sedimentation are clearly attested in Unit C (open- to semi-enclosed marine bay) with local continental influence on the sedimentary processes (rivers or wetlands).

- Unit D, above +4.90 m to +5.20 m a.m.s.l., contains sandy-silty deposits, highly disturbed by anthropogenic activities. Deposition began in the 13th century (after 1221 cal. CE in R6), and these layers contain fragments of marine to lagoonal shells, some pebbles, and occasionally potsherds. Thin coarse sand beds (main mode around 60 µm with one or more coarser secondary modes) are recorded in R4 (at +5.40 m a.m.s.l. and +6.10 m a.m.s.l.).

Units A and B are not recorded in R3, which is located higher in the Rue *foraine*. Nor are they found in R8, which was drilled into what was likely an embankment at the foot of the medieval town fortifications of Rue, according to the map dating from 1640 (Fig. 10b).

4.2. ERT profiles and subsoil resistivity

No archaeological structures were identified in any of the ERT profiles measured northwest of Rue. However, the geophysical survey allows to distinguish three main units, described as follows, from bottom to top (Fig. 5a, 5b, and 5c):

- The geophysical Unit Ge1, with a top depth that varies from 1 m (in ERT4) to ca. 7 m (in R5), has highly variable resistivity values, generally greater than 60 Ωm. According to the reference profiles ERT7 and ERT8, Upper Cretaceous chalk and Pleistocene gravels and pebbles have resistivity values ranging from 40 Ωm to more than 180 Ωm, depending on the degree of weathering of the chalk and the presence (or absence) of groundwater. Comparison of the ERT profiles with the stratigraphy of the cores indicates that the uppermost part of Ge1 consists of Pleistocene gravels and pebbles. The lowermost part is probably composed of chalk. The geometry of this unit is irregular, particularly in ERT4, with a greater depth to the west.
- Unit Ge2, whose thickness varies from a few centimetres (north-northeast of profile ERT4) to about 6 m (southeast of profile ERT3), is characterised by low resistivity (<40 Ωm) related to the finest sedimentary particles (very fine sands of marine or fluvial origin, or organic matter, according to the stratigraphy of R4, R7 and R8). In addition, the conductivity of this unit may have been enhanced by the presence of shallow groundwater, as has been observed in similar sedimentary contexts (Ghilardi et al., 2015, 2017). Ge2 probably corresponds to stratigraphic Units A, B and C.
- Unit Ge3 can be recognized at a depth of *ca.* 2 m in most of the profiles, especially in profiles ERT4, ERT5 and ERT6. It is characterisezd by high resistivity values (from 80 Ωm to *ca*. 300 Ωm). In R4, R7 and R8, the sediments corresponding to this unit are sandy-silty and strongly anthropised (Unit D).

5. Discussion

5.1. Mid- to Late Holocene landscape reconstruction of the Rue area

Palaeogeographical knowledge of the Maye Estuary remains incomplete for the first half of the Holocene. However, the cross combination of geophysical and sedimentological results derived from boreholes helps to partly reveal the palaeorelief. Pleistocene deposits composed of rounded pebbles and blocks ('*Formation de Rue*'; BRGM, 1981) are observed on most of the geophysical (ERT) profiles. Above this presumed marine formation, fine material accumulated (Unit A) within a regional context of marine ingressions, related to the rapid post-glacial sea-

level rise until around 4000 BCE (Garcia-Artola et al., 2018). Our interpretation is strengthened through comparison with core Rue 3 (situated southwest of Rue) as analysed by Ters et al. (1980) (Fig. 1 and 3), who identified and dated foreshore deposits to 4030 ± 240 cal. BCE (after recalibration by Meurisse-Fort, 2007) in the lowermost part of the sedimentary sequence, below a peaty layer. According to Gapenne et al. (2017), the coastal plain was covered by an oak grove around 3000 BCE. These trees slowly disappeared, especially due to the development of bogs.

- From *ca.* 3500 BCE to *ca.* 1000 BCE

Around 3500 BCE, Unit B, defined by the presence of continental peat in several cores, reveals a major environmental change. Back-barrier marshes extended west of the Rue *foraine*. The eastern boundary of this area is influenced by the morphology of the Pleistocene gravel and pebble bar. The ERT profiles performed in the northwest of Rue delineate the upper limit geometry of the deposit of Pleistocene gravels and pebbles, from its outcropping at the top of the Rue *foraine* (eastern ends of ERT6 and NNE of ERT4) to the bottom of adjacent valleys (profile ERT2). Until the beginning of the 3rd millennium BCE, the landscape configuration combined bogs and woodland (Gapenne et al., 2017).

The chronology of peat shows a hiatus between the lowermost part, dated to *ca.* 3500 BCE, and the uppermost part, dated to the late 2nd millennium BCE (Fig. 12a). In addition, the R5 peaty deposit, whose top was dated to *ca.* 1500 BCE, is disrupted by a sandy layer (between +1.25 m a.m.s.l. and +1.50 m a.m.s.l.), probably deposited by storm-surge flooding (see § 5.2).

The upper limit of the peat varies in height, and shows a greater thickness in R4, R5, R6 and R7 than in cores M21 and Rue3 (Lefèvre et al., 1980; Ters et al., 1980), where it was identified around 0 m a.m.s.l. (Figs. 1 and 3). Yet, peat thickness in these cores is very close to that of cores SC1 and SC3, drilled in a small valley south of the Rue *foraine* (Ters et al., 1980). The cores drilled in 2012 reveal conditions that were more sheltered from the sea than those evidenced in cores M21 and Rue3. The local geomorphological context of cores SC1 and SC3 is more similar to that of R4, R5, R6 and R7 (Figs. 1 and 4). These differences confirm the role of the local geomorphological features highlighted by Lefèvre et al. (1980) and Meurisse-Fort (2007), even if sediment compaction probably strongly disturbed the stratigraphy of core Rue3. Comparison between R4, R5, R6 and R7 shows a slight variation in the altitude of the upper limit of the peat. From *ca.* +2.60 m to *ca.* +3 m a.m.s.l., R4 and R7 record the top of Unit B, with finer sediments, including black patches perhaps indicative of old roots, while R5 and R6

show tidal rhythmites similar to those currently observed in the muddy saltmarsh (Smith et al., 1991). Given these features and their location to the southeast of R5 and R6, the area from which R4 and R7 were taken would have been submerged only during high tides and was probably covered by saltmarsh vegetation in *ca.* 1000 BCE (Fig. 12b). In addition, the peat recorded in R6 laminations (Fig. 9) suggests that the area around the core was at the boundary of the high marsh (schorre). In addition, the influence of saltwater inputs on the top of the peaty deposits is proved by a recent analysis of diatoms near the Hère *foraine* (Gapenne et al., 2017).

The relatively recent date (834–752 cal. BCE) and the characteristics of the deposits (dark grey peaty silts) at +1.75 m a.m.s.l. in R6 suggest the influence of human activities on the peatlands at the beginning of the Iron Age. For comparison, large-scale peatland reclamation in the coastal plain of Holland began between 600 and 250 BCE, according to Pierik et al. (2017).

- Around 1000–1250 CE (Fig. 12c)

Human impact (ditches, dikes, fortifications, embankments) on the landscape intensified from at least the 12th century. The sediments recorded between *ca.* +3.90 m and +5 m a.m.s.l. in R4, R5, and R6 (Figs. 6 and 7) continued, nevertheless, to be influenced by marine processes. In these three cores, the sands contain cockle (*Cerastoderma edule*) valves, while the sands in R7 contain land snail fragments that indicate a continental influence of sedimentation. In addition, the thin beds of coarser sand recorded in R4 and R6 at *ca.* +4.30 m a.m.s.l. (Figs. 6 and 7) can be defined as storm surge deposits. The erosional surface (clear contact) between the coarser bed and the underlying marine deposits in R4 testifies to the suddenness of the event (Chaumillon et al., 2017; Pouzet et al., 2018). Moreover, this kind of massive increase in coarser grains (30% of sand and a D_{90} ranging from *ca.* 400 to *ca.* 800 μm) as compared to underlying sediments, has occurred in a similar manner in saltmarsh sediments deposited during recent storm surges (Swindles et al., 2018). The overlying fluvial deposits (Subunit C2) suggest that a fluvial flooding of the area then followed the storm event, which likely occurred in the 12th/13th century BCE, according to the sample dated in R6.

The fine sands (Subunit C3) in R6 between +4.40 m and +5.10 m a.m.s.l. were mainly influenced by human activities. At the same height, the sediments recorded in R4 and, in particular R5, were thinner and even peaty (R5), indicating low energy environments. Mottled sediments (marked by groups of red, yellow and grey patches), between +4.10 m and +4.50 m a.m.s.l. in R5 and between +4.30 m and +5.20 m a.m.s.l. in R4, indicate periodic waterlogging. All these observations suggest that R6 is located near a former river channel that may have been

artificially closed after silting-up. About 100 m to the southeast, R4 is likely situated at the former interface between fresh and saltwater, in the upper part of the muddy flat (slikke) and in an environmental context favourable to cockles (*Cerastoderma edule*). In the area from which R1 and R2 was taken, and where fluvial deposits are recorded, freshwater probably flowed into a natural or artificial channel (ditch).

Wetlands and bogs under continental influence were probably located north and northeast of the former river channel. Freshwater peatlands were identified in sediment cores taken in the 1980s at similar altitudes in other areas to the west, south and southeast of Rue (Lefèvre et al., 1980; Ters et al., 1980). The peat dating performed in R5 at +4.88 m (380–536 cal. CE) conflicts with the datings (989–1052 cal. CE and 1039–1210 cal. CE) obtained for R4 between +4.89 m and +5.12 m a.m.s.l. In addition, the upper peat layer of core M21 analysed by Lefèvre et al. (1980) was dated to 1070 ± 200 CE (Figs. 1 and 3). These results probably indicate that the peat dating obtained for R5 is unreliable, whereas the other two results (in R4) were obtained using charcoal.

The fluvial sediments identified in R1 and R2 (Subunit C2) between +4.50 m and +5 m a.m.s.l. were most likely deposited by the Maye River. The latter, which initially flowed south of the Rue *foraine* in '*le Val de Maye*' (Lefevre et al., 1980; Ters et al., 1980; Fig. 1), moved northwards, probably due to sedimentary deposition at the end of the medieval period. This riverbed change may have been caused by the silting-up of a former pond (called '*étang de Rue*' or '*vivier de Rue*') southeast of Rue, which existed at least from the 13th century CE (Demangeon, 1905) and which had been maintained by dikes downstream. Its siltation may have caused the shift of the Maye towards the northwest, to a channel crossing the Rue *foraine*. In the Late Middle Ages, the channel planform of the Maye was thus similar to today's. The tidal harbour of Rue was established in the upper estuary of this river.

- Since the 13th century CE

Continental processes and human activities have played a major role in the aggradation of the plain since the 13th century. The construction of dikes in the 12th century CE north-northwest of Rue (Briquet, 1930) assisted this aggradation (Unit D).

According to early maps (dating from the late 16th century), the Maye River ended in a closed gulf and Rue was located inland (Fig. 10a). A map from 1773 shows a lock at the mouth of the Maye, at a place called 'la Haie Pénée' approximately 3 km west-southwest of Rue (Fig. 10c), at the boundary of a probable high marsh (schorre). This map also indicates a destroyed dyke ('digue rompue') at the boundary between the saltmarshes and the spring tide line, which

probably corresponds to the limit between high marsh and tidal mudflat. The destroyed dyke also features on the 1758 map by Cassini (Fig. 10d), which confirms the risk of coastal flooding due to dune or dike breaching at that time. Moreover, the Maye canal has carried water from the river towards 'Le Crotoy' since the 1780s, aiding the drainage of the wetlands around Rue.

5.2. Relative sea level changes in the area of Rue during the last 5000 years

The basal part of the peat deposit (Unit B) that overlies an incompressible basement, especially in R5 and R6, can be taken as free basal sea level index points (SLIP), which allow the estimation of past relative sea levels (Brain, 2015; Hijma et al., 2015). Analyses of the peat collected in these cores do not allow us to accurately reconstruct the depositional environment (salinity, in particular) of the peat. Thus, the indicative meaning (the quantitative altitudinal relationship that connected the SLIP with the reference tidal level at the time of deposition; Hijma et al., 2015) of the basal peat of R4, R5, and R6 remains difficult to determine. However, the low concentrations of $CaCO_3$ (<5%) of the peat and the lack of molluscs suggests a predominantly continental influence. This assumption is confirmed by a recent analysis of diatoms collected at the bottom of the peat layer, near the Hère *foraine* (Gapenne et al., 2017). Indeed, we propose to define these indicators as upper limiting data points (Shennan and Horton, 2002; Hijma et al., 2015): under normal conditions, the sea does not reach this limit except, perhaps, during astronomical tides and storm surges. Based on R4, R5, and R6, three limiting points can be defined: (i) 3824–3695 BCE (at +0.90 m a.m.s.l.), (ii) 3798–3654 BCE (at +1.50 m a.m.s.l.), and (iii) 3532–3368 BCE (at +2.10 m a.m.s.l.). Given that the present highest astronomical tide (HAT) is at +6.13 m a.m.s.l. (5.09 m a.m.s.l.), we estimate that:

- at 3824–3695 BCE, the HAT was at *ca.* 0.14 m below the present mean sea level, and the mean sea level was likely around 5.23 m below the present mean sea level.
- at 3798–3654 BCE, the HAT was at *ca.* 0.45 m above the present mean sea level, and the mean sea level was likely 4.63 m below the present mean sea level.
- at 3532–3368 BCE, the HAT was at *ca.* 1.05 m above the present mean sea level, and the mean sea level was likely 4.03 m below the present mean sea level.

These three limiting points and the corresponding probable past mean sea level are in good agreement with the relative sea level evolution over the last 5000 years in Brittany, as reconstructed by Goslin (2014) , even if the HAT indicated by the first limiting data point seems low compared to the second point. The reconstructed relative sea levels are lower than values estimated by the Ice-5G model (Peltier, 2004), and higher than values calculated by the models

603 of Bradley et al. (2011) and Kuchar et al. (2012) (Fig. 11). Our results indicate that the role of
604 tectonic movements in the relative sea level changes over the past 5000 years was insignificant.
605 The faults of the Rue area seem to be inactive.
606
607 The sandy layer recorded at +1.25 m a.m.s.l. and +1.50 m a.m.s.l. in R5 may be explained by
608 storm-surge flooding that was likely linked with major climatic changes identified in north-
609 western Europe (see aforementioned references), particularly 'European Atlantic storm events'
610 (as defined by Pouzet et al., 2018). The shorter second phase of peat accumulation at *ca*. 1300
611 BCE may have been enhanced by the closure of the beach barrier complex. This phase may, in
612 turn, have been stopped by another 'European Atlantic storm event' period that began at *ca.*
613 1100 BCE (Pouzet et al., 2018), as suggested by the clear contact (erosional surface) identified
614 between Unit B and Subunit C1 in R5 at +2.50 m a.m.s.l. (Figs. 7 and 8).
615
616 Regarding the present limit between the slikke and the schorre at *ca.* +4 m a.m.s.l. (Michel et
617 al., 2017), the laminated marine sediments (Subunit C1) situated above the peat sequence in R5
618 and R6, and deposited close to the limit between slikke and schorre at *ca.* 2.70 m a.m.s.l., are
619 probably linked to a sea level, at the beginning of the 1st millennium BCE, of *ca.* 1.30 m below
620 the present one.
621 The coarser sand beds identified in R1, R2, R4, and R6 reflect a greater frequency of marine
622 incursions since *ca.* 1100 CE. Some of these storm surge deposits can be related to the 'EASE
623 1' period (Pouzet et al., 2018) during the early 'Little Ice Age' (in *ca.* 1450 CE), even after land
624 reclamation (as suggested by Lefèvre et al. (1980)) in the area of core M21.
625
626 *5.3. Consequences for human occupation from Neolithic times to the medieval period*
627
628 Our results suggest that the shoreline position was probably located at the foot of the Rue
629 *foraine* at the end of the Middle Neolithic period (*ca*. 3500 BCE). According to Gapenne et al.
630 (2017), at the end of the Neolithic, a forest covered the area. From the end of the Neolithic to
631 the Middle Bronze Age (1600–1350 BCE), much of the lowlands in the area was covered by
632 peatland. Human settlements were probably preferentially located at the top of the Pleistocene
633 bars, at least from the Bronze Age (Rougier, 2012; Gapenne et al., 2017). The lowlands were
634 probably highly exposed to storm surges which, however, did not affect the settlements located
635 on the Pleistocene bars.

From the end of the Bronze Age (*ca.* 1000 BCE) to the Late Middle Ages (987–1492 CE), sediments deposited in the lowlands in the upper part of an estuary were mainly of marine origin. Saltmarshes, including muddy flats (slikke) and high marshes (schorre), developed at the bottom of the Pleistocene bars. During the Iron Age, peatland reclamation may have begun (see § 5.1), but human activities in the lowlands were subject to storm surge flooding.
With the aggradation of the plain and the westward migration of the coastline, the drainage network was shaped.

Finally, despite the lack of archaeological evidence, our results agree well with different historical sources and confirm the likelihood of a coastal harbour at Rue during the 12th and 13th centuries CE; this harbour was probably situated northwest of the town, near '*le Moulin de Saint-Jean*'.

6. Conclusion

Sedimentological analyses derived from boreholes and geophysical investigations conducted in the Rue area, combined with the scrutiny of historical sources have allowed us to reconstruct the Mid- to Late Holocene evolution of the Maye Estuary. The geoarchaeological approach we employ allows to identify: (1) the prevalence of marine environments at the beginning of the 4th millennium BCE, (2) the development of peat accumulation from *ca.* 3500 BCE to the late 2nd millennium BCE, interrupted by a period (between *ca.* 3050 cal. BCE and 1550–1290 cal. BCE) of marine deposition (probably due to storm surges), (3) an estuarine depositional environment around 1000–1250 CE, including a foreshore composed of both mudflats (slikke) and high marshes (schorre) as well as a river channel (Maye), and (4) land reclamation in the former Maye Estuary since the 13th century.
This palaeoenvironmental reconstruction agrees well with recently published sea level curve reconstructions for the Holocene. A continuous Mid- to Late Holocene sea level rise does not conflict with our reconstruction of the Picardy coastal plain evolution.

Based on our results, in around 1000–1250 CE, the town of Rue was bordered to the west by the Maye Estuary, thus confirming literary sources and local legends. The inner estuary was located near '*le Moulin de Saint-Jean'*, where a boat carrying a sacred wooden cross from Jerusalem is reported to have beached during the 12th century. Thus, we suggest that the harbour of Rue was situated northwest of the town, at the upstream boundary of the Maye

Estuary. The creation of an artificial pond southeast of Rue (‘*étang de Rue*’) the diversion of the river towards the medieval town. The discharge of water from the pond to the town was likely caused by anthropic and natural filling in of the wetland. We suggest that this natural barrier was dredged to remove sediments from the harbour and/or to maintain the navigability of the river, as is commonly done today.

Further investigation (coring and geophysical surveys) is required to reconstruct the Holocene evolution of the estuarine landscape to the west and south of Rue. Pollen analyses may also help reconstruct the landuse of the area, in particular during the period of harbour activity of the town.

Acknowledgements

This work was funded by the Regional Council of Picardy from 2011 to 2014. The authors acknowledge Anaïs Doyen, Amandine Gac, Geoffrey Gueit, Rémi Lequint and Mathieu Wawrzyniak for their assistance in field investigations, and thank Rémi Dupuits for his bibliographic study. Laboratory facilities provided by Philippe Racinet (UFR d’Histoire et de Géographie, Université de Picardie Jules-Verne) and Karine Bellart (Service du patrimoine historique de la ville de Rue) were greatly appreciated.

692 **References**

693 Agache, R., Bourdier, R., Petit, P., 1963. Le Quaternaire de la basse Somme : tentative de
694 synthèse. Bull. Soc. Géol. France 7, 422-442.
695 Allen, J.R.M., 2000. Holocene coastal lowlands in NW Europe: Autocompaction and the
696 uncertain ground. In: Pye, K., Allen, J.R.M. (Eds), Coastal and estuarine environments:
697 Sedimentology, geomorphology, and geoarchaeology. The Geological Society of London,
698 London, pp. 239-252. http://dx.doi.org/10.1144/GSL.SP.2000.175.01.18
699 Baeteman, C., Waller, M., Kiden, P., 2011. Reconstructing middle to late Holocene sea-level
700 change: A methodological review with particular reference to 'A new Holocene sea-level
701 curve for the southern North Sea' presented by K.-E. Behre. Boreas 40, 557-572.
702 https://doi.org/10.1111/j.1502-3885.2011.00243.x.
703 Baray, L., 2001. Archéologie funéraire du Bronze ancien au Bronze final en Bourgogne,
704 Franche-Comté, Alsace, Lorraine, Champagne-Ardenne, Île-de-France, Picardie, Pas-de-
705 Calais et Haute-Normandie. Documents d'archéologie méridionale 24, 253-258.
706 Bastide, J., 2011. Morphodynamique et enjeux d'aménagement des franges littorales d'un
707 estuaire macrotidal tempéré : la baie de Somme, Picardie, France. Unp. PhD Thesis,
708 Université du Littoral Côte d'Opale, Dunkerque, 332 p.
709 Beauvais, A, Parisot, J.-C., Savin, C., 2007. Ultramafic rock weathering and slope erosion
710 processes in a south West Pacific tropical environment. Geomorphology 83, 1-13.
711 https://doi.org/10.1016/j.geomorph.2006.06.016.
712 Bellamy, E., Lefebvre, A., Mahe, K., De Rafelis, M., 2009. Croissance de la coque
713 (Cerastoderma edule) en baie de Somme : Morphométrie et Marquage. RST/LER.BL/09.04.
714 https://archimer.ifremer.fr/doc/00007/11815/
715 Ben Redjeb, T., Foucray, B. 1989. Découverte d'un dépôt monétaire gallo-romain à Rue
716 (Somme) ; premières données. Revue archéologique de Picardie 3-4, 87-91.
717 Bengtsson, L., Enell, M., 1986. Chemical analysis. In Berglund B.E. (Eds.) Handbook of
718 Holocene Palaeoecology and Palaeohydrology, John Wiley & Sons, Chichester, p. 423-451
719 Bradley, S., Milne, G.A., Shennan, I., Edwards, R., 2011. An improved Glacial Isostatic
720 Adjustment model for the British Isles. Journal of Quaternary Science 26 (5), 541-552.
721 https://doi.org/10.1002/jqs.1481.
722 Brain, M. J., 2015. Compaction. In: Shennan, I., Long, A.J., Horton, B.P. (Eds.), Handbook of
723 Sea-Level Research. Wiley Blackwell, Hoboken, pp. 52-469.
724 https://doi.org/10.1002/9781118452547.ch30

Brain, M.J., Long, A.J., Petley, D.N., Horton, B.P., Allison, R.J., 2011. Compression behaviour of minerogenic low energy intertidal sediments. Sedimentary Geology 233, 28-41. https://doi.org/10.1016/j.sedgeo.2010.10.005.

BRGM (with the collaboration of Menessier, G., Lefèvre, P., Monliardini, C., Auffret, J.-P., Agache, R.), 1981. Rue. Carte géologique de la France au 1/50 000 n°23. BRGM, Orléans, 14 p.

BRGM (with the collaboration of Broquet, P., Auffret, J.-P., Beun, N., Dupuis, C., Monliardini, C., Agache R.), 1985. St-Valéry-sur-Somme/Eu. Carte géologique de la France au 1/50 000 n°31-32. BRGM, Orléans, 38 p.

Briquet, A., 1930. Le littoral du Nord de la France et son évolution morphologique, Armand Colin, Paris, 483 p.

Bungenstock, F., Weerts, H.J.T., 2010. The high-resolution Holocene sea-level curve for Northwest Germany: global signals, local effects or data-artefacts? International Journal of Earth Sciences (Geologische Rundschau) 99, 1687-1706. https://doi.org/10.1007/s00531-009-0493-6

Buurman, P., de Boer, K., Pape, T., 1997. Laser Diffraction grainsize characteristics of Andisols in perhumid Costa Rica: The aggregate size of allophane. Geoderma 78, 71-91. https://doi.org/10.1016/S0016-7061(97)00012-8.

Buurman, P., Pape, T., Muggler, R.C.C., 1996. Laser grain-size determination in soil genetic studies: Practical problems. Soil Science 162, 211-218. 10.1097/00010694-199703000-00007.

Chaumillon, E., Bertin, X., Fortunato, A., Bajo, M., Schneider, J.L., Dezileau, L., Michelot, A., Chauveau, E., Créach, A., Hénaff, A., Walsh, J.P., Sauzeau, T., Waeles, B., Gervais, B., Jan, G., Baumann, J., Breilh, J.F., Pedreros, R., 2017. Storm-induced marine flooding: lessons from a multidisciplinary approach. Earth-Science Reviews 165, 151-184. https://doi.org/10.1016/j.earscirev.2016.12.005.

Clarke, M. L., Rendell, H. M., 2009. The impact of North Atlantic storminess on western European coasts: A review. Quaternary International 195, 31-41. https://doi.org/10.1016/j.quaint.2008.02.007.

Clavé, B., Massé, L., Carbonel, P., Tastet, J.-P., 2001. Holocene coastal changes and infilling of the La Perroche marsh (French Atlantic coast). Oceanologica Acta 24 (4), 377-389. https://doi.org/10.1016/S0399-1784(01)01153-7.

Costa, S., Suanez, S., 2013. Géomorphologie des littoraux français. In: Mercier, D. (Ed.), Géomorphologie de la France. Dunod, Paris, pp. 65-77.

759 Daire, M.-Y., Dupont, C., Baudry, A., Billard, C., Large, J.-M., Lespez, L., Normand, E.,
760 Scarre, C, 2013. Ancient maritime communities and the relationship between people and
761 environment along the European Atlantic coasts, British Archeological Reports,
762 Archaeopress, Oxford, 320 p.
763 Dalrymple, R.W., Zaitlin, B.A., Boyd, R., 1992. Estuarine facies models: conceptual basis and
764 stratigraphic implications. Journal of Sedimentary Research 62 (6), 1130-1146.
765 https://doi.org/10.1306/D4267A69-2B26-11D7-8648000102C1865D
766 Dark, P., 2006. Climate deterioration and land-use change in the first millennium BC:
767 perspectives from the British palynological record. Journal of Archaeological Science 33,
768 1381-1395. https://doi.org/10.1016/j.jas.2006.01.009.
769 Dean, W.E., 1974. Determination of carbonate and organic matter in calcareous sediments and
770 sedimentary rocks by loss on ignition: Comparison with other methods. Journal of
771 Sedimentary Petrology 44, 242-248. https://doi.org/10.1306/74D729D2-2B21-11D7-
772 8648000102C1865D.
773 Delaporte, E., 1925. Quelques mots sur l'histoire de Rue, Imprimerie du Marquenterre E.
774 Dumont, Rue, 165 p.
775 Demangeon, A., 1905. La Picardie et les régions voisines. Artois, Cambrésis, Beauvaisis, Thèse
776 de doctorat. Armand Colin, Paris, 496 p.
777 Dobroniak, C., 2000. Géomorphologie, hydrodynamique et écologie d'un estuaire tempéré
778 macrotidal : l'Authie, Manche orientale, France. Unp. PhD Thesis, Université du Littoral
779 Côte d'Opale, Dunkerque, 308 p.
780 Flucher, G., 2004. Rue, Bastion Saint-Jean. In: Direction régionale des Affaires Culturelles
781 Picardie. Service Régional de l'Archéologie. Bilan scientifique 2004, pp. 120-121.
782 Gandouin, E., 2003. Enregistrement paléoclimatique de la transgression Holocène ; signature
783 paléoenvironnementale des Chironomidae (Diptères) du bassin de Saint-Omer (France).
784 Unp. PhD Thesis, Université des sciences et technologies, Lille, 256 p.
785 Gandouin, E., Van Vliet-Lanoë, B., Franquet, E., Andrieu-Ponel, V., Keen, D.H., Ponel, P.,
786 Meurisse, M., Brulhet, J., Brocandel, M., 2007. Analyse en haute résolution de la
787 transgression holocène dans un secteur subsident du littoral français : le bassin-marais de St
788 Omer (Pas de Calais, France). Géologie de la France, 2007 (1), 11-32.
789 Gapenne, A., Barbet, P., Rannou, J.-C., Béthune, B., Bouet, C., Jouanin, G., Boulen, M.,
790 Buchez, N., Canny, D., Coutard, S., Ducrocq, T., Durin, C., Flahaut, J., Vincent, V., Gonnier,
791 C., Hugonnier, L., Lancelot, S., Lecomte-Schmitt, B., Mariette, E., Vacossin, J.-F. Rue,

792 “Foraine de Hère”, “carrière d'Hère-les-Rue” 2017 (Somme). Rapport de fouilles. INRAP,
793 Paris, 584 p.
794 Garcia-Artola, A.G., Stephan P., Cearreta A., Kopp R.E., Khan N.S., Horton B.P., 2018.
795 Holocene sea-level database from the Atlantic coast of Europe. Quaternary Science Reviews
796 196, 177-192. https://doi.org/10.1016/j.quascirev.2018.07.031.
797 Ghilardi, M., Psomiadis, D., Pavlopoulos, K., Müller-Celka, S., Fachard, S., Theurillat, T.,
798 Verdan, S., Knodell, A., Theodoropoulou, T., Bicket, A., Bonneau, A., Delanghe-Sabatier,
799 D., 2014. Mid- to Late Holocene shoreline reconstruction and human occupation in Ancient
800 Eretria (South Central Euboea, Greece). Geomorphology 208, 225-237.
801 https://doi.org/10.1016/j.geomorph.2013.12.006.
802 Ghilardi, M., Istria, D., Curras, A., Vacchi, M., Contreras, D., Vella, C., Dussoulliez, P., Crest,
803 Y., Guiter, F., Delanghe, D., 2017. Reconstructing the landscape evolution and the human
804 occupation of the Lower Sagone River (Western Corsica, France) from the Bronze Age to
805 the Medieval period. Journal of Archaeological Science: Reports, 12, 741-754.
806 https://doi.org/10.1016/j.jasrep.2016.07.009.
807 Ghilardi, M., Sanderson, D., Kinnaird, T., Bicket, A., Balossin, S., Parisot, J.-C., Hermitte, D.,
808 Guibale, F., Fleury, J.T., 2015. Dating the Bridge at Avignon (South France) and
809 reconstructing the Rhone River fluvial palaeo-landscape in Provence from Medieval to
810 Modern times. Journal of Archaeological Science: Reports 4, 336-354.
811 https://doi.org/10.1016/j.jasrep.2015.10.002.
812 Goffé, B., Guérin, R., Mercier, E., Lœuille, N., Pubellier, M., 1998. Le contrôle tectonique de
813 la morphologie de la baie de Somme. Ses conséquences sur la sédimentation. In: Hoeblich,
814 J.-M. (Éd.), Colloque La baie de Somme en question, Amiens 3/11/98, pp. 25-32.
815 Goslin, J., 2014. Reconstitution de l’évolution du niveau marin relatif holocène dans le Finistère
816 (Bretagne, France) : dynamiques régionales, réponses locales. Unp. PhD Thesis, Université
817 de Bretagne Occidentale, Brest, 355 p.
818 Goslin, J., Van Vliet-Lanoë, B., Stéphan, P., Delacourt, C., Fernane, A., Gandouin, E., Hénaff,
819 A., Penaud, A., Suanez, S., 2013. Holocene relative sea-level changes in western Brittany
820 (France) between 7600 and 4000 cal. BP: Reconstitution from basal-peat deposits.
821 Géomorphologie : relief, processus, environnement 19 (4), 425-444.
822 10.4000/geomorphologie.10386
823 Hijma, M.P., Engelhart, S.E., Törnqvist, T.E., Horton, B.P., Hu, P., Hill, D.F., 2015. A Protocol
824 for a Geological Sea-Level Database. In: Shennan, I., Long, A.J., Horton, B.P. (Eds),

825 Handbook of Sea-Level Research. Wiley Blackwell, Hoboken, pp. 536-553.
826 https://doi.org/10.1002/9781118452547.ch34
827 Horton, B.P.; Shennan, I., 2009. Compaction of Holocene strata and the implications for relative
828 sealevel change on the east coast of England. Geology 37 (12), 1083-1086.
829 https://doi.org/10.1130/G30042A.1
830 Kuchar, J., Milne, G., Hubbard, A., Patton, H., Bradley, S.L., Shennan, I., Edwards, R.J., 2012.
831 Evaluation of a numerical model of the British-Irish ice sheet using relative sea-level data:
832 implications for the interpretation of trimline observations. Journal of Quaternary Science
833 27, 597-605. https://doi.org/10.1002/jqs.2552.
834 Labrecque, C., 2008. La chapelle du Saint-Esprit de Rue, Picardie, étude historique,
835 architecturale et iconographique d'un monument de la fin du Moyen Age. Unp. PhD Thesis,
836 Université Laval, Québec, 608 p.
837 Lefèvre, P., Rouvillois, A., Gaffet M.-A., Bignot, G., 1980. Alternances de sédimentation
838 marine et continentale durant l'Holocène en plaine maritime picarde. Bulletin de
839 l'Association française pour l'étude du Quaternaire 17 (1-2), 25-33.
840 10.3406/quate.1980.1365
841 Le Fournier, J., 1974. La sédimentation Holocène en bordure du littoral picard et sa signification
842 dynamique. Bull. Centre Rech. Explor. Prod. Elf Aquitaine 8 (1), 327-349.
843 Le Fournier, J., 1980. Modern analogue of transgressive Sand bodies off eastern English
844 Channel. Bull. Centre Rech. Explor. Prod. Elf Aquitaine 4 (1,), 99-118.
845 Lequint, R., Fouache, E., 2012. Apports de la géoarchéologie à l'étude de la baie de Wissant
846 (Pas-de-Calais, France). Ann. Soc. Géol. du Nord 19 (2ème série), 1-4.
847 Lespez, L., Clet-Pellerin, M., Davidson, R., Marcigny, C., Levalet, F., Hardel, B., 2004.
848 Evolution des paysages et anthropisation depuis le Néolithique dans la péninsule de La
849 Hague. Revue d'Archéométrie 28, 71-88. 10.3406/arsci.2004.1063
850 Lespez, L., Clet-Pellerin, M., Davidson, R., Hermier, G, Carpentier, V., Cador, J.-M., 2010.
851 Middle to Late Holocene landscape changes and geoarchaeological implications in the
852 marshes of the Dives estuary (NW France). Quaternary International 216 (1-2) 23-40.
853 https://doi.org/10.1016/j.quaint.2009.06.018.
854 Loke, M.H., 2003. RES2DINV, Rapid 2-D Resistivity and IP Inversion Using the Least-Square
855 Method (Geotomo doftware User's Manual). Geotomo Software, Singapore, 123 p.
856 Long, A.J., Hughes, P.D.M., 1995. Mid- and late-Holocene evolution of the Dungeness
857 foreland, UK. Marine Geology 124, 253-271. https://doi.org/10.1016/0025-3227(95)00044-
858 Y.

859 Long, A.J., Waller, M.P., Stupples, P., 2006. Driving mechanisms of coastal change: Peat
860 compaction and the destruction of late Holocene coastal wetlands. Marine Geology 225, 63-
861 84. https://doi.org/10.1016/j.margeo.2005.09.004.
862 Louandre, F.-C., 1844-1845. Histoire d'Abbeville et du comté de Ponthieu jusqu'en 1789.
863 Joubert, Paris; Jeunet, Abbeville 2 vol.
864 Marion, C., Anthony, E.J., Trentesaux, A., 2009. Short-term (<2 yrs) estuarine mudflat and
865 saltmarsh sedimentation: High-resolution data from ultrasonic altimetery, rod surface-
866 elevation table, and filter traps. Estuarine, Coastal and Shelf Science 83, 475–484.
867 doi:10.1016/j.ecss.2009.03.039
868 Meurisse, M., Van Vliet-Lanoë, B., Talon, B., Recourt, P., 2005. Complexes dunaires et
869 tourbeux holocènes du littoral du Nord de la France. C. R. Geoscience 337, 675-684.
870 10.1016/j.crte.2005.02.009.
871 Meurisse-Fort, M., 2007. Enregistrement haute résolution des massifs dunaires. Manche, mer
872 du Nord et Atlantique : le rôle des tempêtes. Unp. PhD Thesis, Université de Lille 1, 306 p.
873 Michel, C., 2016. Morphodynamique et transferts sédimentaires au sein d'une baie mégatidale
874 en comblement (Baie de Somme, Manche Est). Stratégie multi-échelles spatio-temporelles.
875 Unp. PhD Thesis, Normandie Université, 409 p.
876 Michel, C., Le Bot, S., Druine, F., Costa, S., Levoy, F., Dubrulle-Brunaud, C., Lafite, R., 2017.
877 Stages of sedimentary infilling in a hypertidal bay using a combination of sedimentological,
878 morphological and dynamic criteria (Bay of Somme, France). Journal of Maps 13 (2), 858-
879 865. 10.1080/17445647.2017.1389
880 Moura, D., Veiga-Pires, L., Albardeiro, T., Boski, T., Rodrigues, A.L., Tareco, H., 2007.
881 Holocene sea level fluctuations and coastal evolution in the central Algarve (southern
882 Portugal). Marine Geology 237, 127-142. https://doi.org/10.1016/j.margeo.2006.10.026.
883 Mrani-Alaoui, M., Anthony, E. J., 2011. New data and a morphodynamic perspective on mid-
884 to late-Holocene palaeoenvironmental changes in the French Flanders coastal plain, southern
885 North Sea. The Holocene 21 (3), 445-453. https://doi.org/10.1177/0959683610385724.
886 Munaut, A.V., Gilot, E., 1977. Recherches palynologiques et datations 14C dans les régions
887 côtières du nord de la France : Phases transgressives et stabilisations dunaires flandriennes
888 dans l'estuaire de la Canche (Pas de Calais). Bull. Ass. Fr. Et. Quat. 14 (3), 17-25.
889 Notte, L., 2002. Rue. La Foraine bleue. In: Direction régionale des affaires culturelles Picardie.
890 Service régional de l'archéologie (Eds.), Bilan scientifique 2002, pp. 122-123.
891 Pailler, Y., Stéphan, P., Gandois, H., Nicolas, C., Sparfel, Y., Tresset, A., Klet, D., Fichaut, B.,
892 Suanez, S., Dupont, C., Le Clézio, L., Marcoux, N., Pineau, A., Salanova, L., Sellami, F.,

Debue, K., Josselin, J., Dietsch-Sellami, M.-F., 2011. Evolution des paysages et occupation humaine en mer d'Iroise (Finistère, Bretagne) du Néolithique à l'Âge du Bronze. Norois 220, 39-68. 10.4000/norois.3662.

Peltier, W.R., 2004. Global Glacial Isostasy and the Surface of the Ice-Age Earth: The ICE-5G (VM2) Model and GRACE. Annual Review of Earth and Planetary Science 32, 111-149. https://doi.org/10.1146/annurev.earth.32.082503.144359.

Pierik, H.J., Cohen, K.M., Vos, P.C., van der Spek, A.J.F., Stouthamer, E., 2017. Late Holocene coastal-plain evolution of the Netherlands: the role of natural preconditions in human-induced sea ingressions. Proceedings of the Geologists' Association 128, 180-197. https://doi.org/10.1016/j.pgeola.2016.12.002.

Poiret, E., 1931. Essai sur la topographie et l'aspect de Rue au milieu du XVe siècle, Bulletin de la Société historique du Canton de Rue, Rue, E. Dumont, pp.5-20.

Pontee, N., Tastet, J.P., Massé, L., 1998. Morphosedimentary evidence of Holocene coastal changes near the mouth of the Gironde and on the Medoc Peninsula, S.W. France. Oceanologica Acta 21 (2), 243-261. https://doi.org/10.1016/S0399-1784(98)80012-1.

Pouzet, P., Maanan, M., Piotrowska, N., Baltzer, A., Stéphan, P., Robin, M., 2018. Chronology of Holocene storm events along the European Atlantic coast: new data from the island of Yeu, France. Prog. Phys. Geogr.: Earth Environ. 42, 431-450. https://doi.org/10.1177/0309133318776500.

Quesnel, Y., Jrad, A., Mocci, F., Gattacceca, J., Mathé, E., Parisot, J.-C., Hermitte, D., Dumas, V., Dussouillez, P., Walsh, K., Miramont, C., Bonnet, S., Uehara, M., 2011. Geophysical signatures of a Roman and Early Medieval Necropolis. Archaeological Prospection 18, 105-115. https://doi.org/10.1002/arp.411.

Reimer, P.J., Bard, E., Bayliss, A., Beck, J.W., Blackwell, P.G., Bronk Ramsey, C., Buck, C.E., Cheng, H., Edwards, R.L., Friedrich, M., Grootes, P.M., Guilderson, T.P., Haflidason, H., Hajdas, I., Hatté, C., Heaton, T.J., Hoffmann, D.L., Hogg, A.G., Hughen, K.A., Kaiser, K.F., Kromer, B., Manning, S.W., Niu, M., Reimer, R.W., Richards, D.A., Scott, E.M., Southon, J.R., Staff, R.A., Turney, C.S.M., van der Plicht, J., 2013. IntCal13 and MARINE13 radiocarbon age calibration curves 0–50000 years cal. BP. Radiocarbon 55 (4), 1869–1887. https://doi.org/10.2458/azu_js_rc.55.16947.

Ritz, M., Parisot, J.-C., Diouf, S., Beauvais, A., Diome, F., Niang, M., 1999. Electrical imaging of lateritic weathering mantles over granitic and metamorphic basement of eastern Senegal, West Africa. Journal of Applied Geophysics 41, 335-344. https://doi.org/10.1016/S0926-9851(99)00008-7.

927 Rougier, R., 2012. Rue (Somme), La foraine de Hère, Carrière d'Hère-lès-Rue, Rapport de
928 diagnostic. INRAP, Paris, unpublished, 129 p.
929 Rougier, R., Blancquaert, G., 2001. Un établissement rural de La Tène Dl à Rue « Le Chemin
930 des Morts » (Somme). Revue archéologique de Picardie 3 (4), 81-104.
931 Rougier, R., Hosdez, C., Chaidron, C., Ben Redjeb, T., Thuet, A., 2008. Une fouille préventive
932 à Quend « Le Muret » (Somme) : questions sur l'organisation et le rôle d'un site côtier au
933 Bas-Empire. Revue archéologique de Picardie 3 (1), 203-246. 10.3406/pica.2008.3141.
934 Service hydrographique et océanographique de la marine (SHOM), 2017. Références
935 altimétriques maritimes. Ports de France métropolitaine et d'outre-mer. Côtes du zéro
936 hydrographique et niveaux caractéristiques de la marée, Edition 2017. 118 p.
937 Shennan, I., Horton, B.P., 2002. Holocene land- and sea-level changes in Great Britain. J. Quat.
938 Sci. 17, 511-526. https://doi.org/10.1002/jqs.710.
939 Shennan, I., Bradley, S. L., Edwards, R., 2018. Relative sea-level changes and crustal
940 movements in Britain and Ireland since the Last Glacial Maximum. Quaternary Science
941 Reviews 188, 143-159. https://doi.org/10.1016/j.quascirev.2018.03.031.
942 Siart, C., Hecht, S., Holzhauer, I., Altherr, R., Meyer, H.P., Schukraft, G., Eitel, B., Bubenzer,
943 O., Panagiotopoulos, D., 2010. Karst depressions as geoarchaeological archives: the
944 palaeoenvironmental reconstruction of Zominthos (Central Crete) based on geophys-ical
945 prospection, mineralogical investigations and GIS. Quat. Int. 216, 75–92.
946 0.1016/j.jasrep.2016.07.009
947 Smith, D.G., Reinson, G.E., Zaitlin, B.A., Rahmani, R.A., 1991. Clastic Tidal Sedimentology.
948 Can. Soc. Pet. Geol. Mem. 16, 387 p.
949 SOGREAH, 1995. Étude sédimentologique de la Baie de Somme. Rapp. Conseil Général de la
950 Somme, 65 p.
951 Sorrel, P., Debret, M., Billeaud, I., Jaccard, S.L., McManus, J.F., Tessier, B., 2012. Persistent
952 non-solar forcing of Holocene storm dynamics in coastal sedimentary archives. Nature
953 Géoscience 5, 892-896. https://doi.org/10.1038/ngeo1619
954 Stéphan, P., 2011. Colmatage sédimentaire des marais maritimes et variations relatives du
955 niveau marin au cours des 6 000 dernières années en rade de Brest (Finistère). Norois 220,
956 9-37. 10.4000/norois.3659
957 Stéphan, P., Goslin, J. 2016. Évolution du niveau marin relatif à l'Holocène le long des côtes
958 françaises de l'Atlantique et de la Manche : réactualisation des données par la méthode des
959 "sea-level index points", Quaternaire 25 (4), 295-312. 10.4000/quaternaire.7261

960 Stuiver, M., Reimer, P.J., 1993. Extended ^{14}C data base and revised CALIB 3.0 ^{14}C age
961 calibration program. In: Stuiver, M., Long, A., Kra, R.S. (Eds.), Calibration 1993.
962 Radiocarbon, 35 (1), pp. 215-230. 10.1017/S0033822200013904
963 Swindles, G.T., Galloway, J.M., Macumber, A.L., Croudace, I., Emery, A.R., Woulds, C.,
964 Bateman, M.D., Parry, L., Jones, J.M., Selby, K., Rushby, G.T., Baird, A.J., Woodroffe,
965 S.A., Barlow, N.L.M., 2018. Sedimentary records of coastal storm surges: evidence of the
966 1953 North Sea event. Marine Geology 403 (1), 262-270. 10.1016/j.margeo.2018.06.013
967 Tastet, J.-P., Pontee, N.I., 1998. Morpho-chronology of coastal dunes in Medoc. A new
968 interpretation of Holocene dunes in Southwestern France. Geomorphology 25 (1-2), 93-109.
969 10.1016/S0169-555X(98)00035-X
970 Ters, M., 1973. Les variations du niveau marin depuis 10 000 ans, le long du littoral atlantique
971 français. In: Le Quaternaire : géodynamique, stratigraphie et environnement : travaux
972 français récents. 9e congrès international de l'INQUA, Christchurch, Décembre 1973.
973 Comité National Français de l'INQUA, Paris, pp. 114-135.
974 Ters, M., 1986. Variations in Holocene sea level on the french Atlantic coast and their climatic
975 significance. In: Rampino, M.R., Sanders, J.E., Newman, W.S., Königsson, L.K. (Eds.),
976 Climate: history, periodicity and predictability. Van Nostrand Reinhold, New York, pp. 204-
977 237.
978 Ters, M., Delibrias, G., Denèfle, M., Rouvillois, A., Fleur, A. 1980. Sur l'évolution
979 géodynamique du Marquenterre (Basse-Somme) à l'HoIocène et durant le Weichsélien
980 ancien. Bulletin de l'Association française pour l'étude du Quaternaire 17 (1-2), 11-23.
981 10.3406/quate.1980.1364
982 Tessier, B., Billeaud, I, Sorrel, P., Delsinne, N, Lesueur, P., 2012. Infilling stratigraphy of
983 macrotidal tide-dominated estuaries. Controlling mechanisms: Sea-level fluctuations,
984 bedrock morphology, sediment supply and climate changes (The examples of the Seine
985 estuary and the Mont-Saint-Michel Bay, English Channel, NW France). Sedimentary
986 Geology 279, 62-73. 10.1016/j.sedgeo.2011.02.003
987 Trentesaux, A., Margotta, J., Le Bot, S., 2012. The Somme bay, NW France: a wave-dominated
988 macrotidal estuary? In: The 8th International Conference on Tidal Environments. Tidalites
989 2012. Publication of the French Association of Sedimentologists 72. Paris, 40 p.
990 Van Vliet-Lanoë, B., Goslin, J., Hallegouët, B., Henaff, A., Delacourt, C., Fernane, A.,
991 Franzetti, M., Le Cornec, E., Le Roy, P., Penaud, A., 2014a. Middle- to late-Holocene
992 storminess in Brittany (NW France): Part I – morphological impact and stratigraphical
993 record. The Holocene 24 (4), 413-433. 10.1177/0959683613519687

994 Van Vliet-Lanoë, B., Penaud, A., Henaff, A., Delacourt, C., Fernane, A., Goslin, J., Hallegouët,
995 B., Le Cornec, E., 2014b. Middle- to late-Holocene storminess in Brittany (NW France):
996 Part II – The chronology of events and climate forcing. The Holocene 24 (4), 434-453.
997 10.1177/0959683613519688
998 Vink, A., Steffen, H., Reinhardt, L., Kaufmann, G., 2007. Holocene relative sea-level change,
999 isostatic subsidence and the radial viscosity structure of the mantle of northwest Europe
1000 (Belgium, the Netherlands, Germany, southern North Sea). Quaternary Science Reviews 26,
1001 3249-3275. 10.1016/j.quascirev.2007.07.014
1002
1003

Figure and table captions

Fig. 1: Location and Geological maps of the study area

1: Spot height (in meters); 2: '*Plateau Picard*': Upper Cretaceous chalk with flints; 3: Flint pebble spit; 4: Holocene dunes and sand bars; 5: '*Formation du Marquenterre*': Holocene clay and sands; 6: Holocene alluvial deposits; 7: Holocene peat; 8: '*Formation de Rue*': Pleistocene pebble spit; 9: Fault; 10: Hidden fault; 11: River; 12: Location of corings undertaken by Lefèvre et al. (1980) and Ters et al. (1980) **(**source: BD ORTHO® IGN, 2017; BRGM)

Fig. 2: Comparison between the Holocene sea level curves proposed by Meurisse-Fort (2007) and Mrani-Alaoui and Anthony (2011)

1: Sea level curves estimated with radiocarbon-dated peat and palaeosol samples (Mrani-Alaoui and Anthony, 2011); 2: Sea level curves from Belgium (Mrani-Alaoui and Anthony, 2011); 3: High tide level curve proposed by Meurisse-Fort (2007)

Fig. 3: Comparative sections of five corings, South of Rue (Somme)

1: Chalk; 2: Chalky loam, with pieces of flint and sand; 3: Pleistocene gravels (rounded flint pebbles in a matrix of fine sand; 4: Loam with fine layers of peat; 5: Peat; 6: Clay or loam; 7: Loamy silts; 8: Marine sands; 9: Marine sandy silts; 10: Shell debris; 11: Dating – a: 2910 ± 90 BP according to Ters et al. (1980)/1110 ± 210 cal. BCE according to Meurisse-Fort (2007); b: 4650 ± 150 BP/3450 ± 190 cal. BCE; c: 5220 ± 110 BP/4030 ± 240 cal. BCE; d: 980 ± 100/1070 ± 200 cal. BCE; e: 3060 ± 110 BP/1270 ± 270 cal. BCE; f: 5080 ± 140 BP/3940 ± 300 cal. BCE; g: 5520 ± 150 BP/4370 ± 330 cal. BCE; h: 6450 ± 160 BP/5350 ± 320 cal. BCE

Fig. 4: ERT profiles and drill core locations. Map based on BD ORTHO® (source: IGN, 2017) and RGE ALTI® 1m (source: IGN, 2017)

Fig. 5a: ERT2, ERT4, ERT5, and ERT6 profiles (2D view) and identified geoelectric units (Ge)

Cores R4, R7 and R8 are reported in the corresponding sections and the reader can refer to the description of the sedimentary units.

Fig. 5b: ERT1, and ERT3 profiles (2D view) and identified geoelectric units (Ge)

Cores R1, R2 and R7 are reported in the corresponding sections and the reader can refer to the description of the sedimentary units.

Fig. 5c: ERT7, and ERT8 profiles (2D view) and identified geoelectric units (Ge)

Fig. 6: Chronostratigraphy of cores R1, R2, R3, and R4

Organic matter, carbonate content and granulometric indices (mean and mode) are reported for each core, plotted as a function of depth below the surface.

1: Heterogeneous sand; 2: Heterogeneous sand with gravels and pebbles; 3: Heterogeneous deposit with sand (medium to coarse), pebbles and shell fragments; 4: Coarse sand; 5: Medium sand; 6: Very fine to fine sand; 7: Tidal rhythmites; 8: Silty sand; 9: Peaty silt; 10: Peat including plant debris; 11: Weathered chalk; 12: Mottled sediments (with red, yellow and grey spots); 13: >35 % calcium carbonate content surficial deposits; 14: Potsherds; 15: Cockle fragments (*Cerastoderma edule*); 16: Snail fragments; 17: Colluvium; 18: Clear contact; 19: AMS radiocarbon dating; 20: Subunit M1; 21: Subunit M2: 22: Unit P; 23: Subunit Ch; 24: Subunit Cm; 25: Subunit Cf; 26: Unit H

Fig. 7: Chronostratigraphy of cores R5, R6, R7, and R8

Organic matter, carbonate content and granulometric indices (mean and mode) are reported for each core, plotted as a function of depth below the surface.

1: Heterogeneous sand; 2: Heterogeneous sand with gravels and pebbles; 3: Heterogeneous deposit with sand (medium to coarse), pebbles and shell fragments; 4: Coarse sand; 5: Medium sand; 6: Very fine to fine sand; 7: Tidal rhythmites; 8: Silty sand; 9: Peaty silt; 10: Peat including plant debris; 11: Weathered chalk; 12: Mottled sediments (with red, yellow and grey spots); 13: >35 % calcium carbonate content surficial deposits; 14: Potsherds; 15: Cockle fragments (*Cerastoderma edule*); 16: Snail fragments; 17: Colluvium; 18: Clear contact; 19: AMS radiocarbon dating; 20: Subunit M1; 21: Subunit M2: 22: Unit P; 23: Subunit Ch; 24: Subunit Cm; 25: Subunit Cf; 26: Unit H

Fig. 8: Chronostratigraphic cross-section based on drilled cores

1: Heterogeneous sand; 2 : Heterogeneous sand with gravels and pebbles; 3: Heterogeneous deposit with sand (medium to coarse), pebbles and shell fragments; 4: Coarse sand; 5: Medium sand; 6: Very fine to fine sand; 7: Tidal rhythmites; 8: Silty sand; 9: Peaty silt; 10: Peat including plant debris; 11: Mottled sediments (with red, yellow and grey patches); 12: >35 % calcium

carbonate content surficial deposits; 13: Potsherds; 14: Cockle fragments (*Cerastoderma edule*); 15: Snail fragments; 16: Colluvium; 17: Clear contact; 18: AMS radiocarbon dating

Fig. 9: Tidal rhythmites recorded in core R6 (between 2.57 and 2.82 m depth).

Fig. 10: Examples of old maps of the Rue area

9a: Detail of the map drawn in 1579 by J. Surhonio *'Picardiae, Belgicae regionis descriptio, Joanne Surhonio auctore. Cum Imp. et Reg. privilegio decenn. 1579. Ponthiev, Santerre, Vermandois, Terrache, Tartenois, Cambresis, Vimevx, Beauvois, Laonnois, Baillage de Hesdin, Artésia, Champagnae, Hannoniae'* (Departmental Archives of the Somme: 1FI956). The town of Rue is indicated by a yellow circle.

9b: *'Plan des fortifications de la ville de Rue en 1640'* (Departmental Archives of the Somme: 1FI285). The brown circles indicate the location of R3 and R8.

9c: Detail of the map drawn in 1773 *'Plan des différents canaux tant de navigation que de dessèchement projettés dans le terrain situé entre l'embouchure des rivières de Somme, de Maye et d'Authie'* (National Archives: N III Somme 8-2). The town of Rue is marked with a red circle. The lock at 'la Haie Pénée' is indicated by a solid blue circle; the destroyed dyke downstream is indicated by a dotted blue circle.

9d: Detail of a map published in 1758 under the direction of César-François Cassini de Thury *'Carte générale de la France ; 023. [Dieppe]. N°23. 15e Flle'* (https://www.geoportail.gouv.fr). The town of Rue is indicated by a red circle.

Fig. 11: Comparison between the past mean sea level reconstructed in the Rue area, the sea level index point identified in Brittany (France) by Goslin (2014), and glacial isostatic adjustment models

1: Basal peats identified by Goslin (2014); 2: Intercalated sea level index points identified by Goslin (2014); 3: Limiting points identified by Goslin (2014); 4: Limiting points defined in our study (HAT: reconstructed highest astronomical tide; msl: probable mean sea level); 5: Current sea level (HAT: highest astronomical tide; msl: mean sea level); 6: Ice-5G model (Peltier, 2004); 7: Bradley et al. (2011) model; 8: Kuchar et al. (2012) model.

Fig. 12: Palaeogeographic reconstruction of the northwest of the Rue area from *ca.* 1300 BCE

12a—1: Rue *foraine*; 2: Swampy area; 12b—1: Rue *foraine*; 2: High marsh (schorre); 3: Mudflat (slikke); 12c—1: Rue *foraine*; 2: Coast; 3: Maye estuary; 4: Limit of the medieval town of Rue; 5: Present channel of the Maye; 6: Probable former channel of the Maye

Table 1: ERT profile locations

Table 2: Radiocarbon dating results

Figure

Click here to access/download;Figure;Fig1.jpg

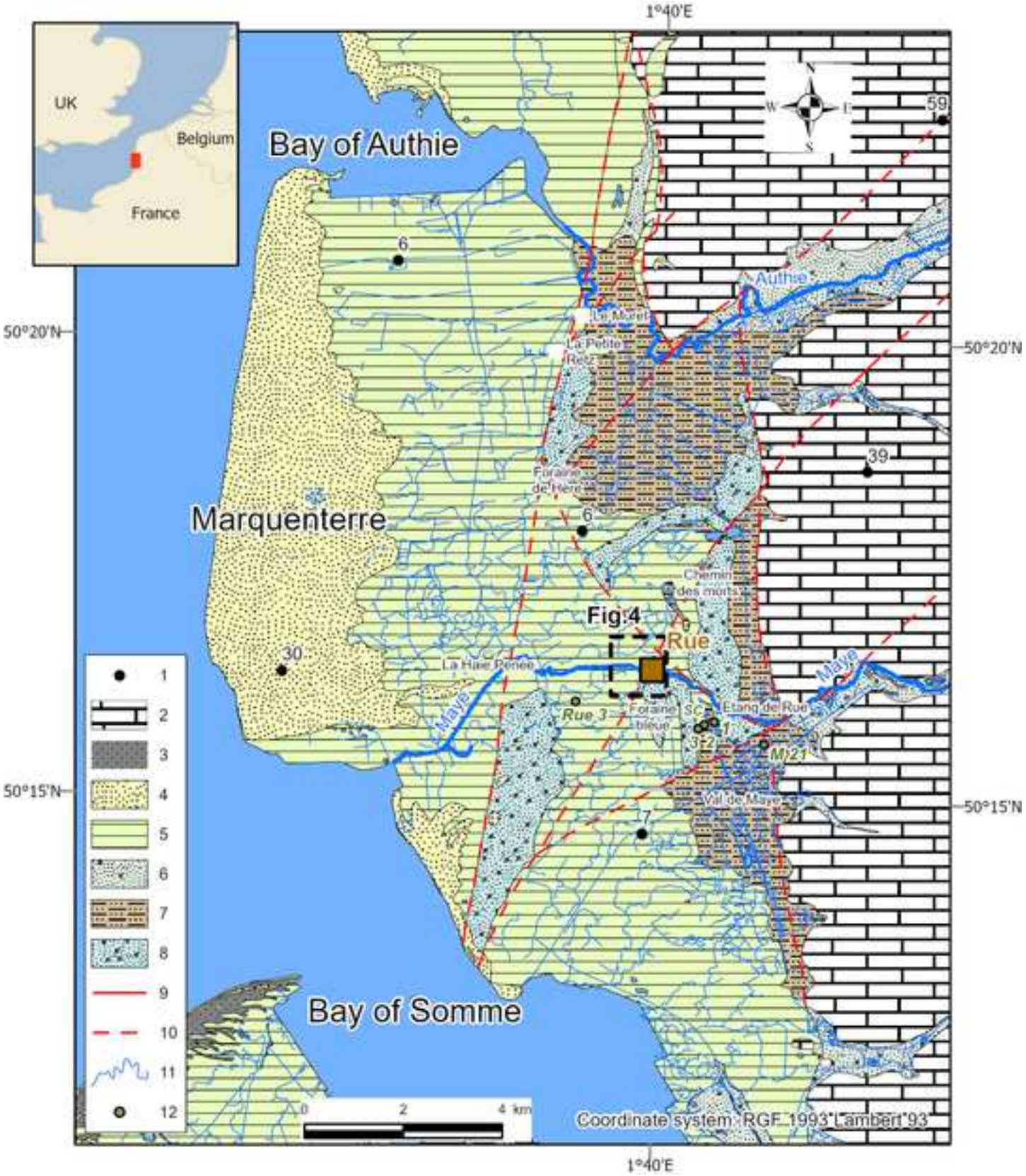

Figure

Click here to access/download;Figure;Fig2.jpg

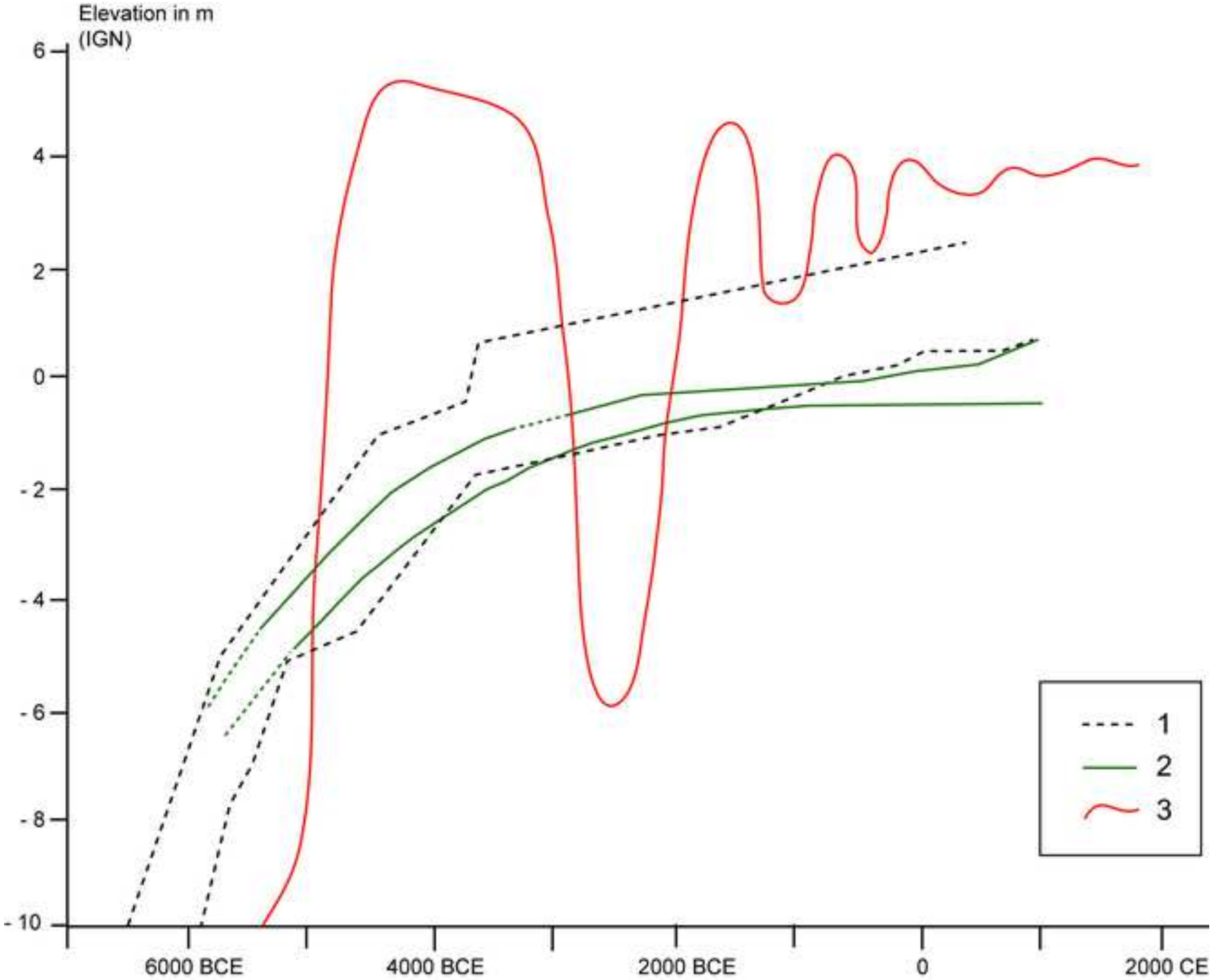

Figure

Click here to access/download;Figure;Fig3.jpg

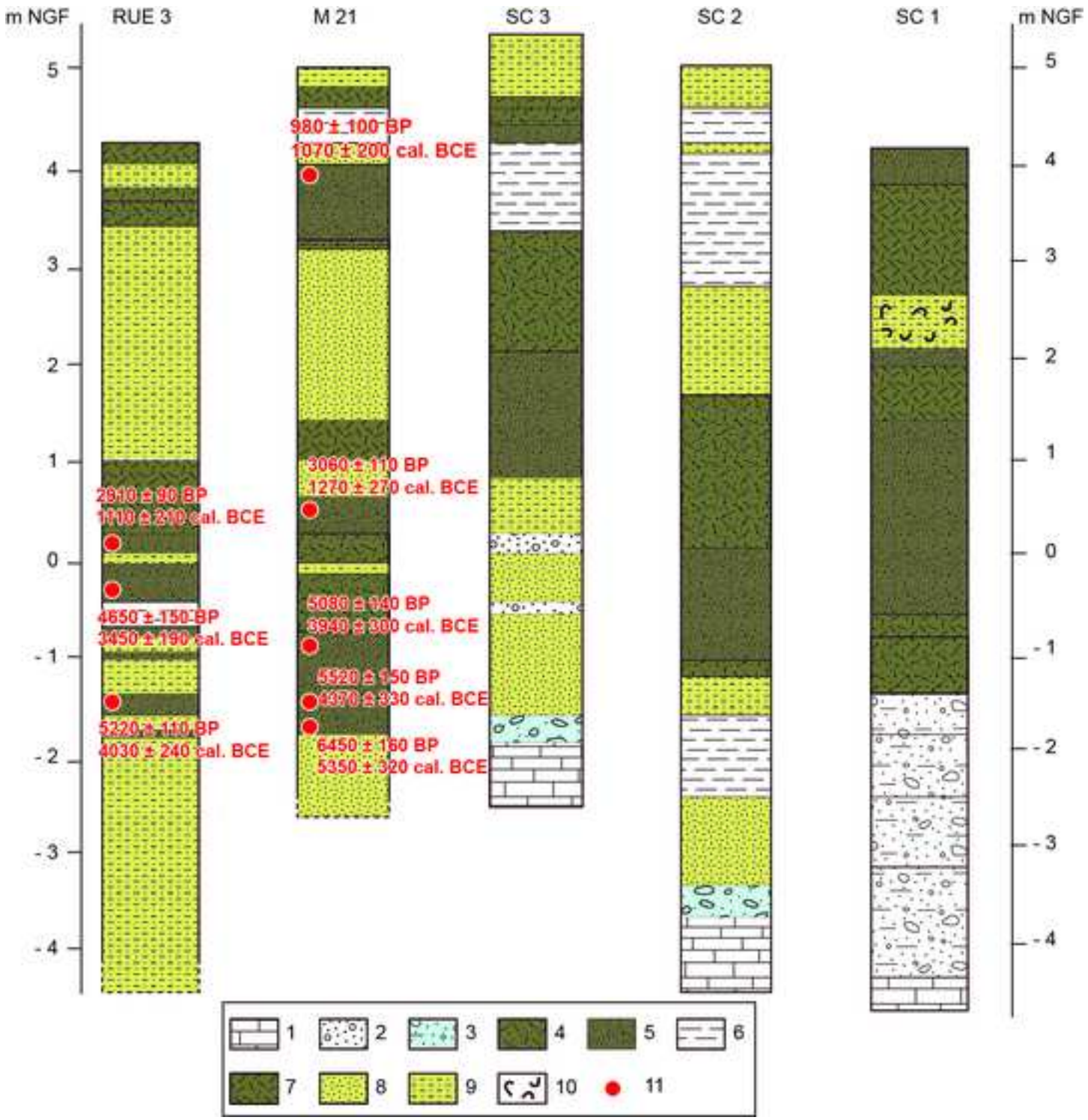

Figure

Click here to access/download;Figure;Fig4.jpg

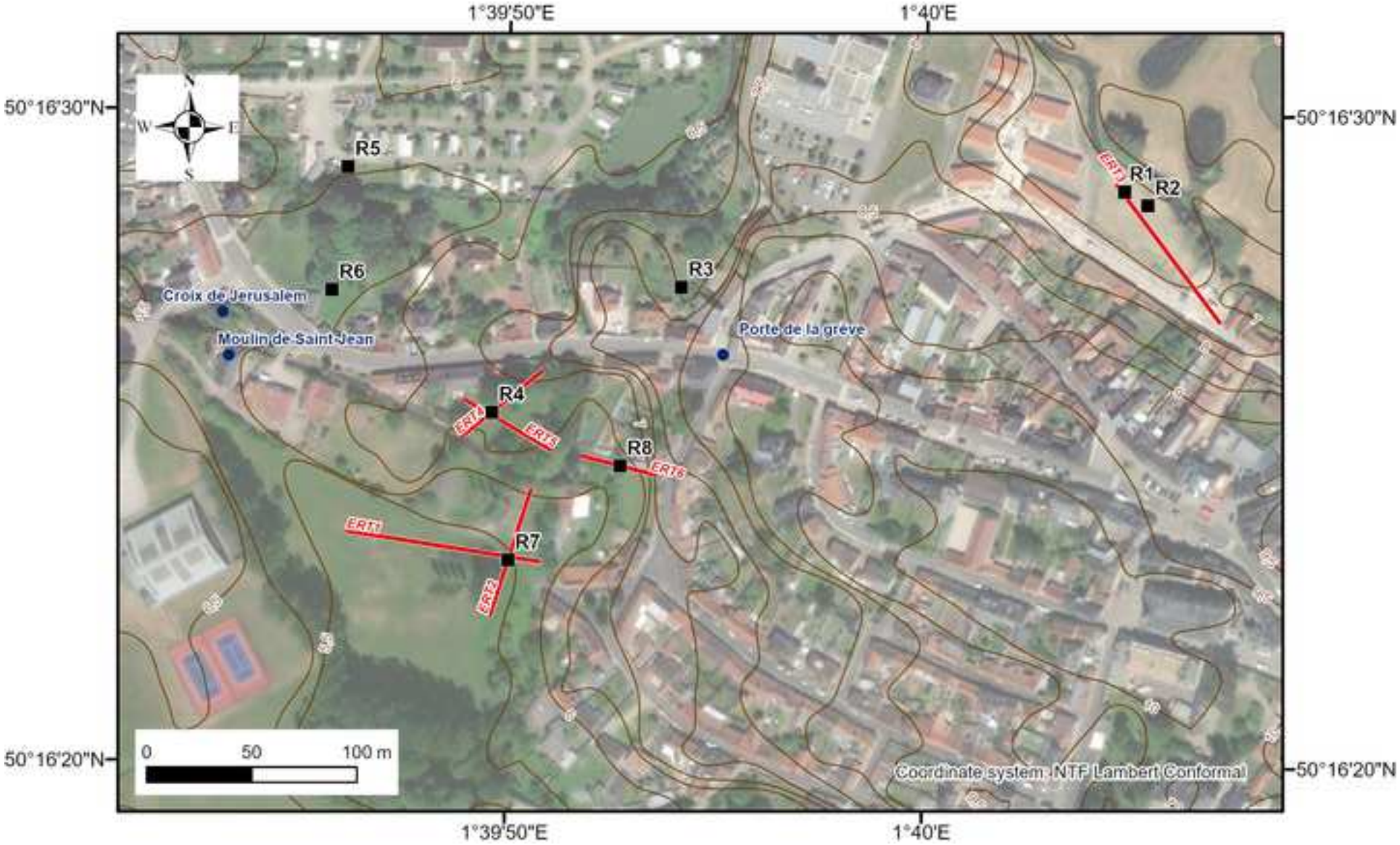

Figure

Click here to access/download;Figure;fig5a.jpg

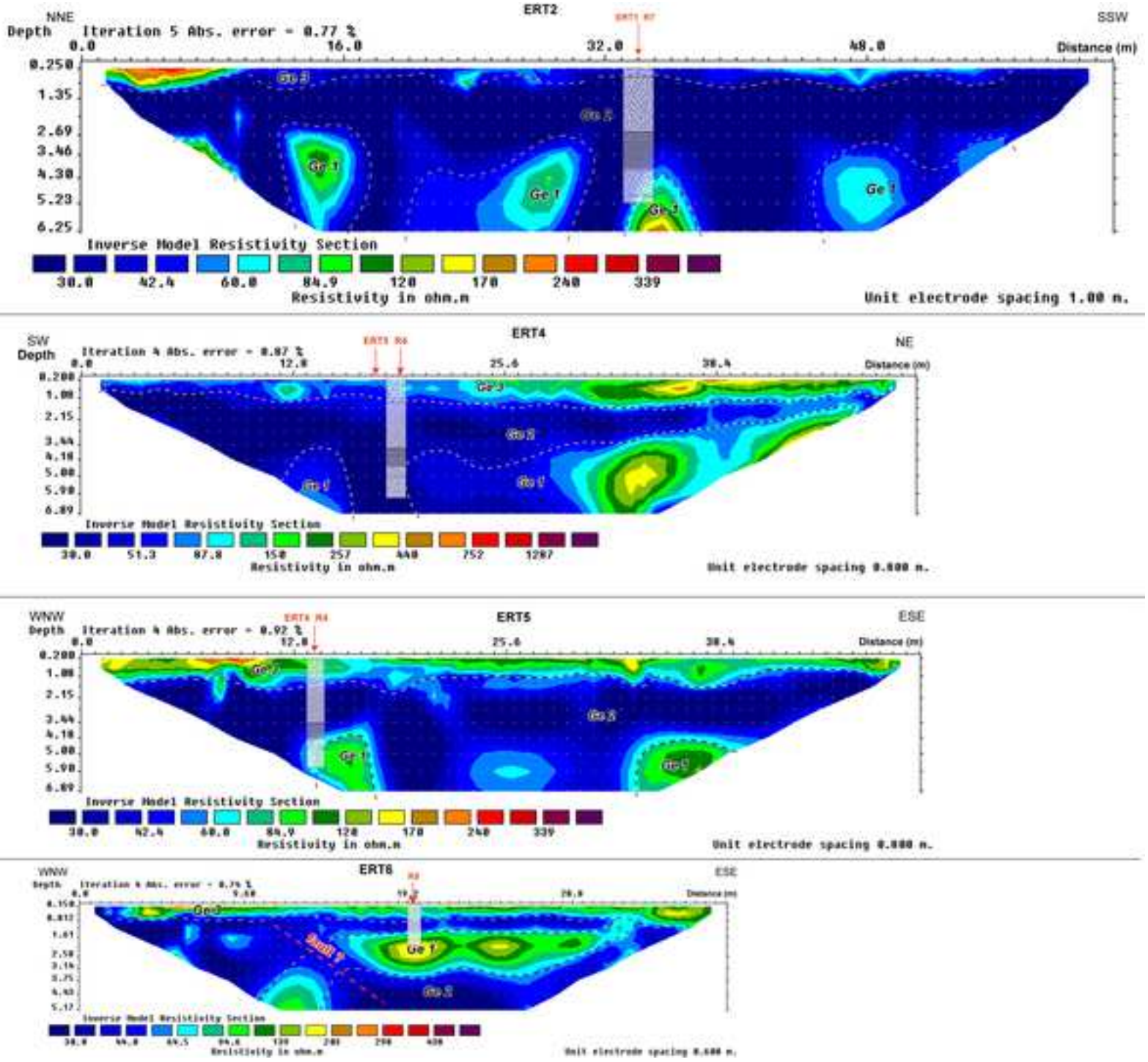

Figure

Click here to access/download;Figure;fig5b.jpg

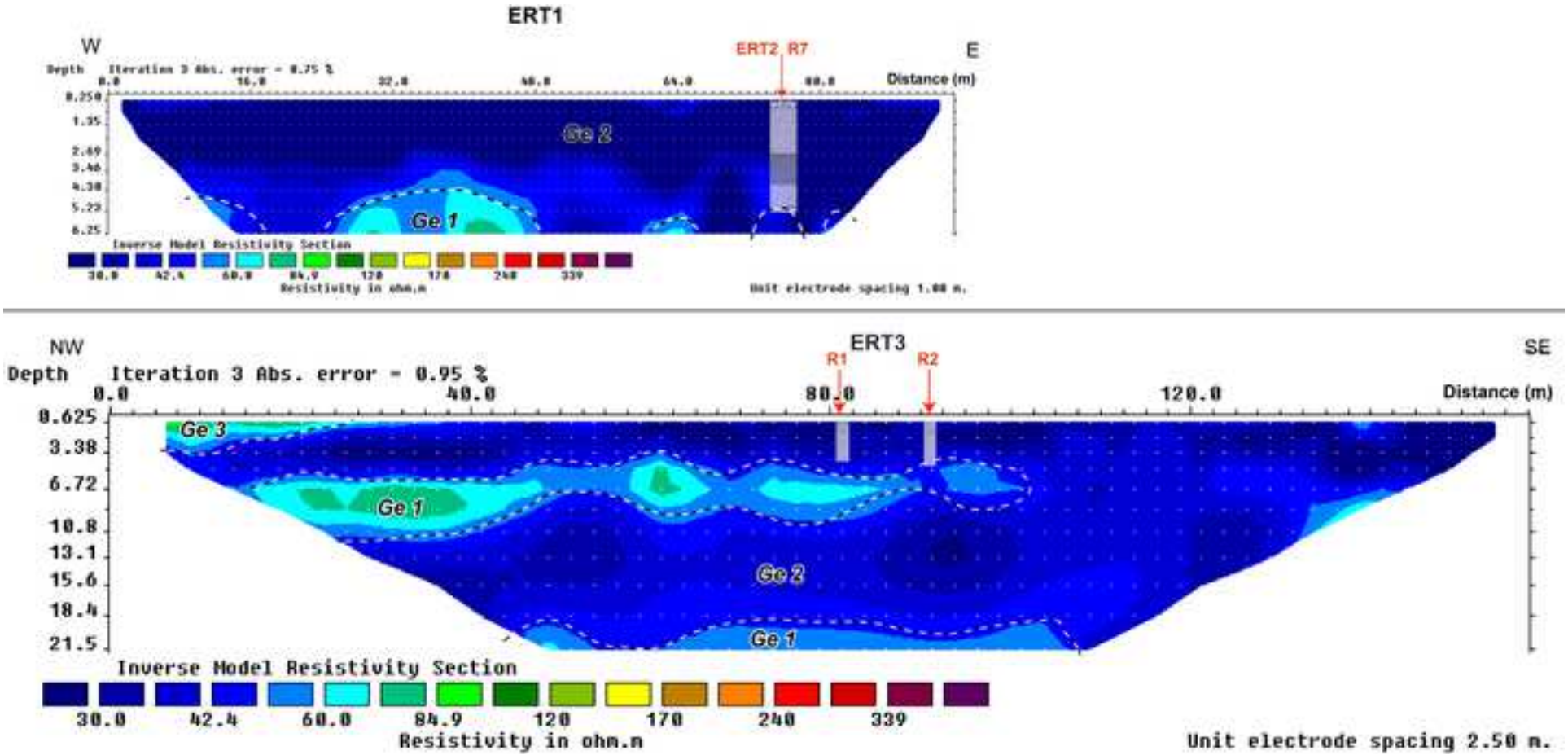

Figure

Click here to access/download;Figure;fig5c.jpg

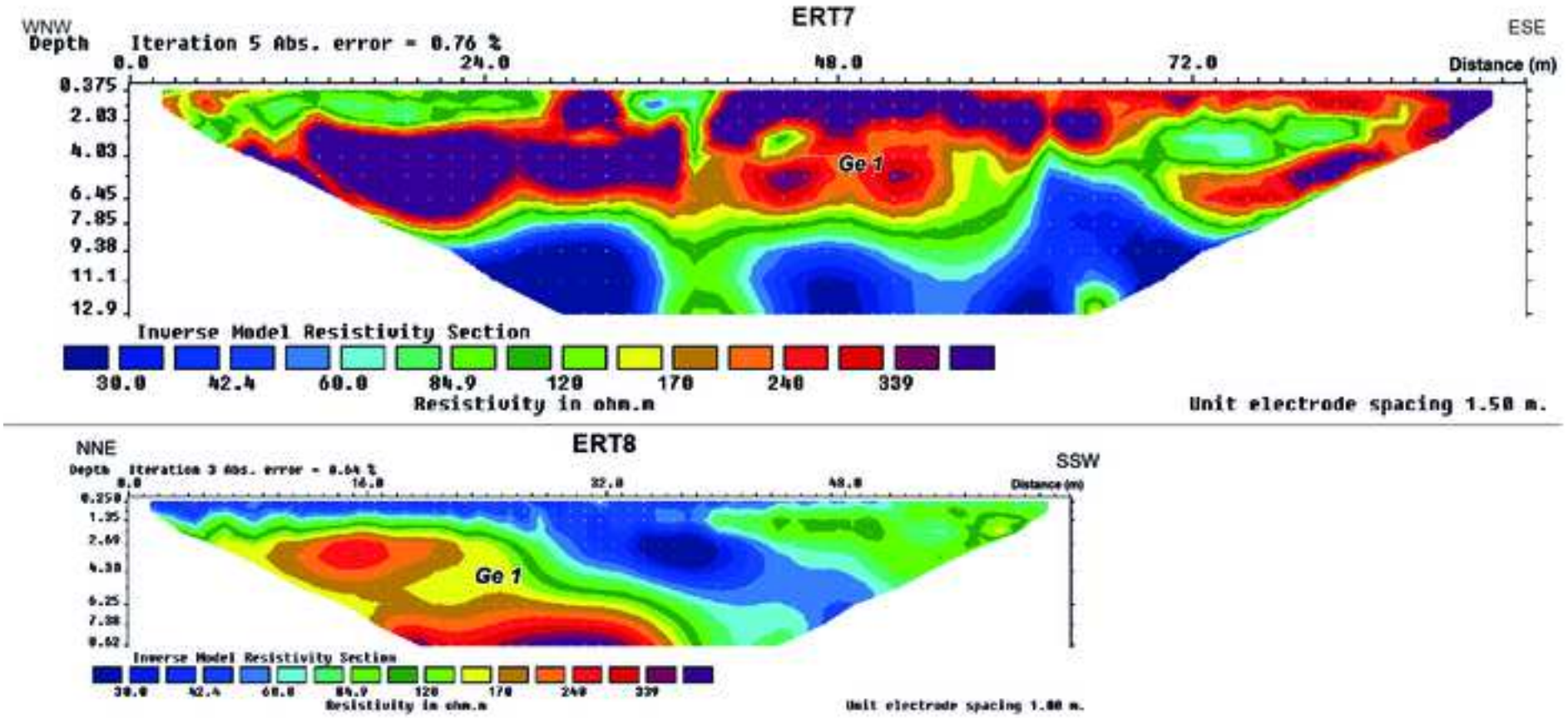

Figure

Click here to access/download;Figure;fig6.jpg

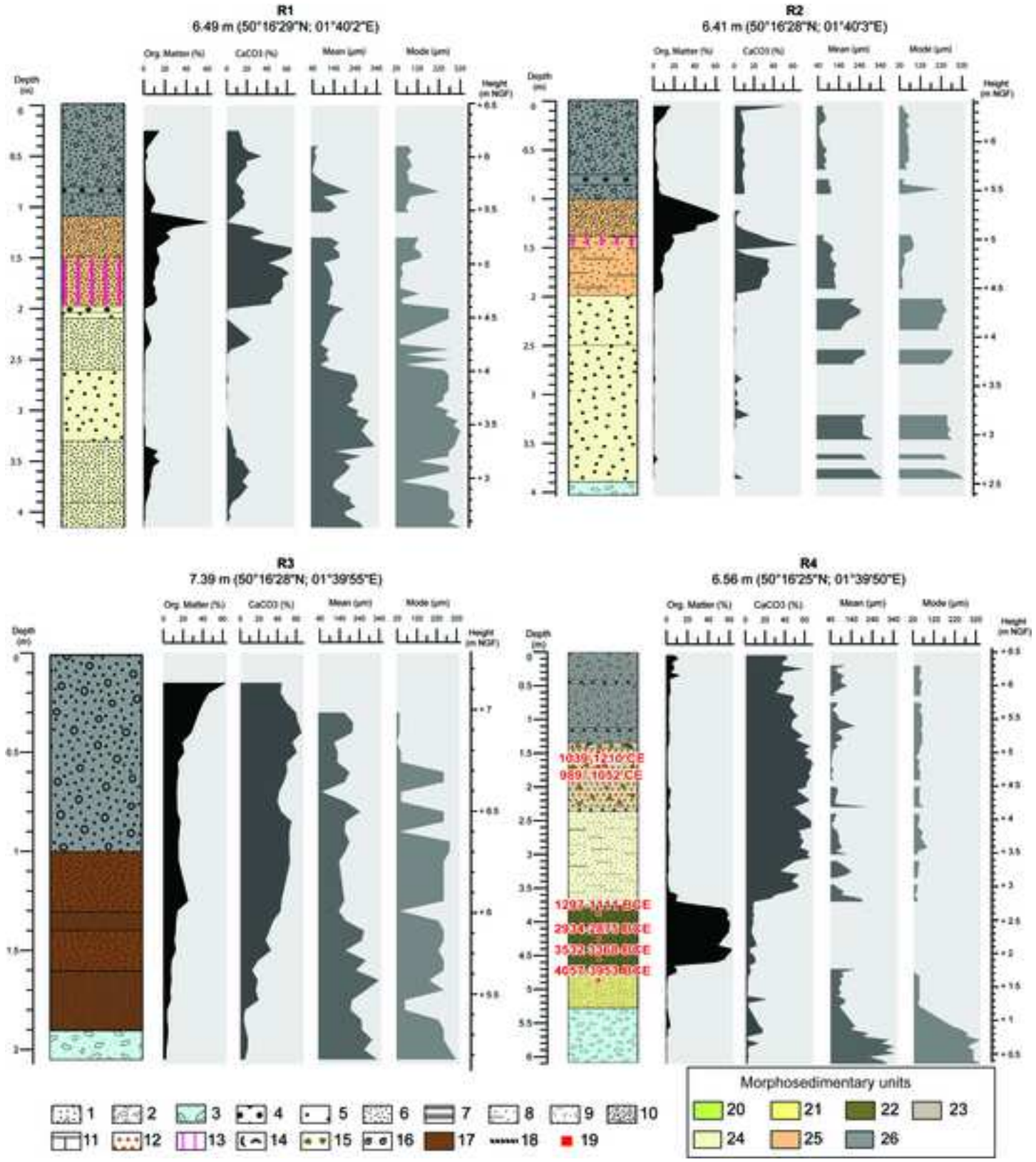

Figure

Click here to access/download;Figure;Fig7.jpg

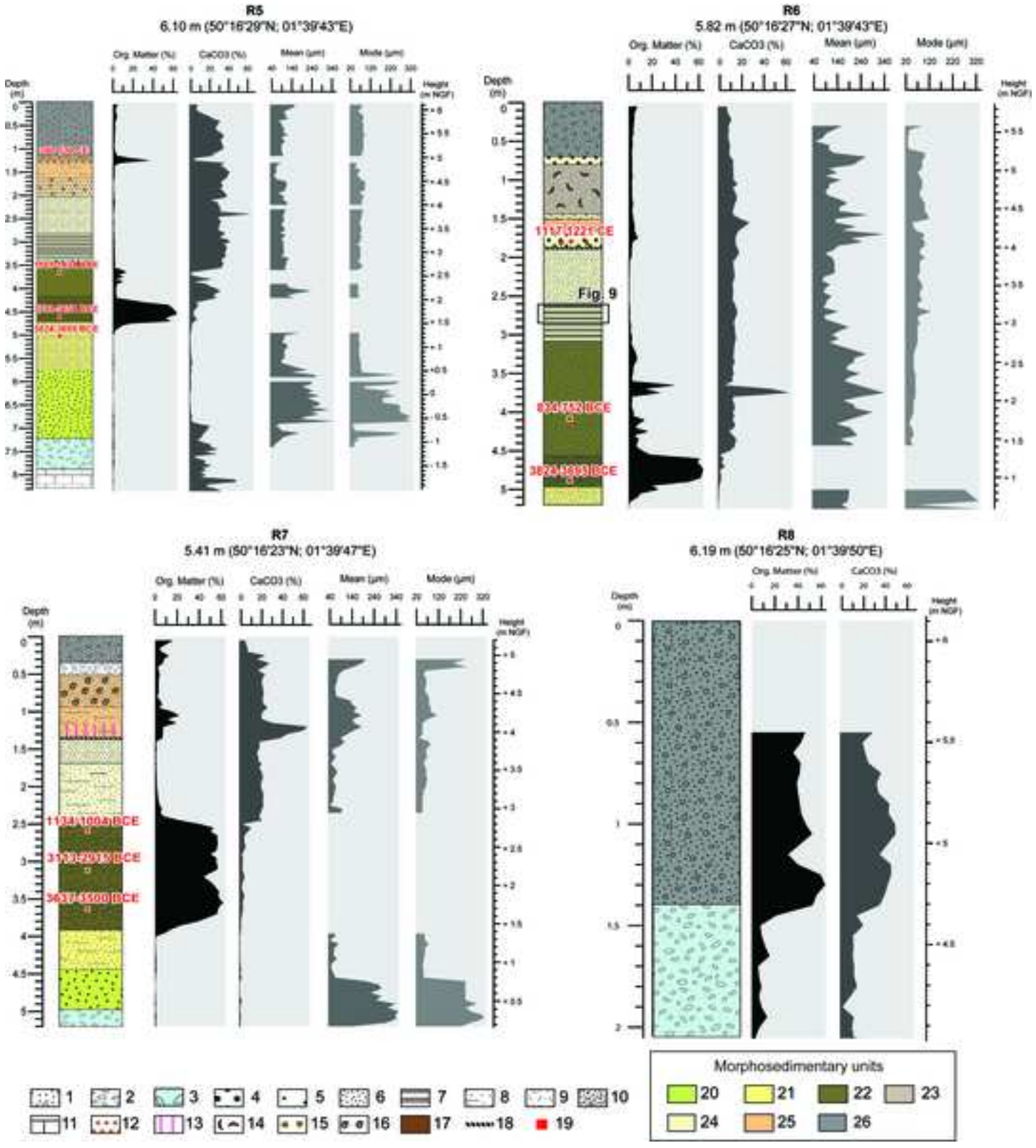

Figure

Click here to access/download;Figure;Fig8.jpg

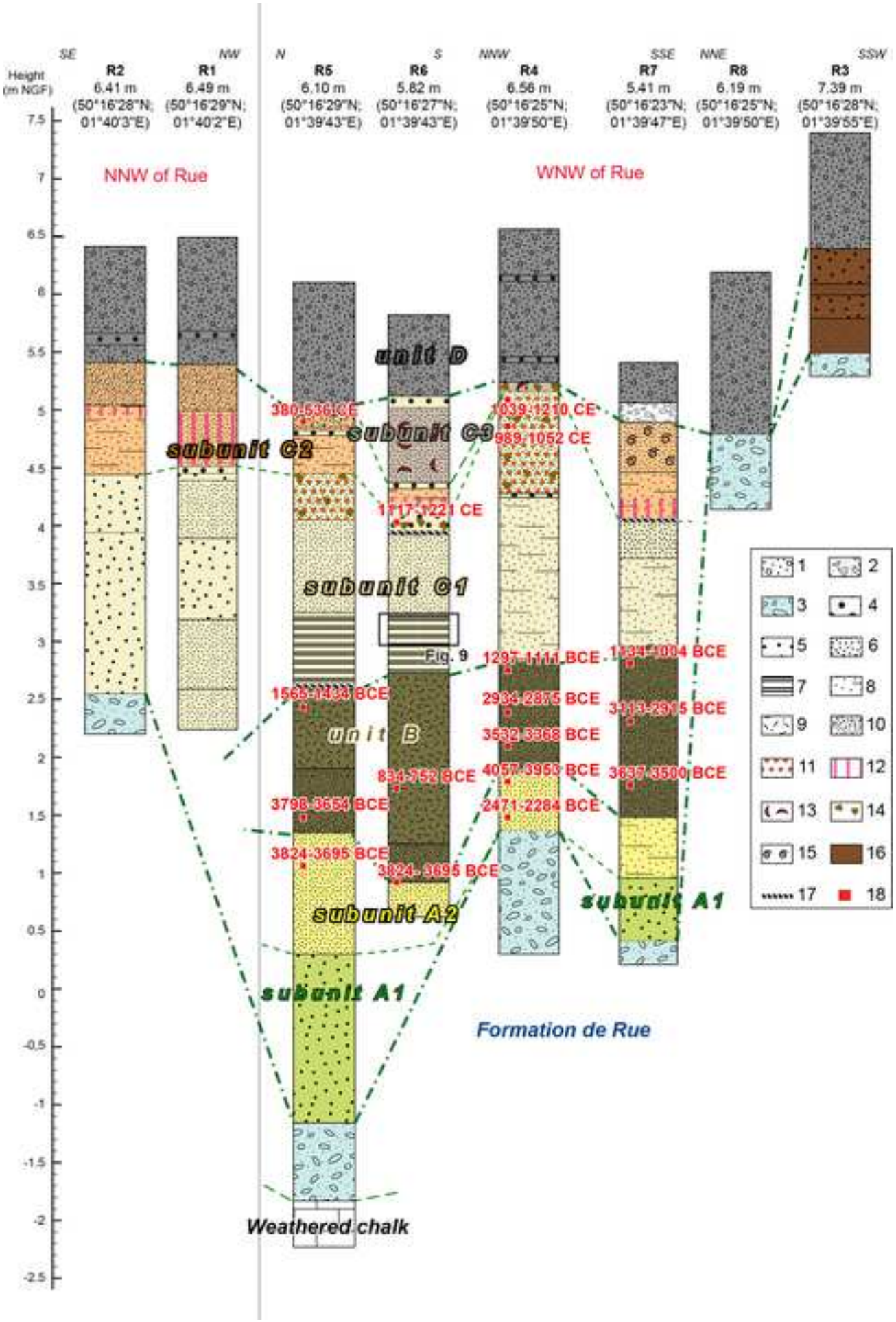

Figure

Click here to access/download;Figure;fig9.jpg

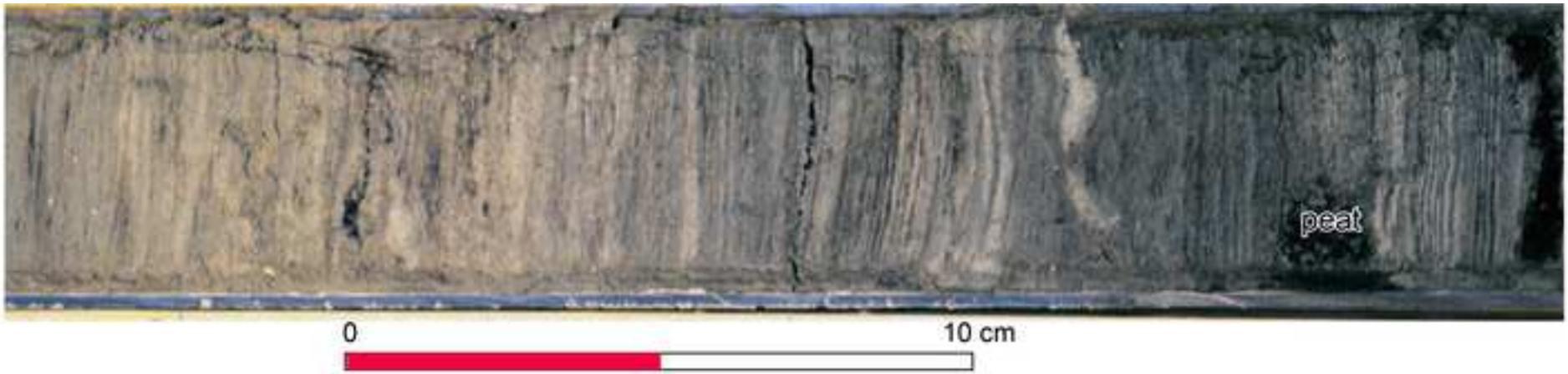

Figure

Click here to access/download;Figure;Fig10.jpg

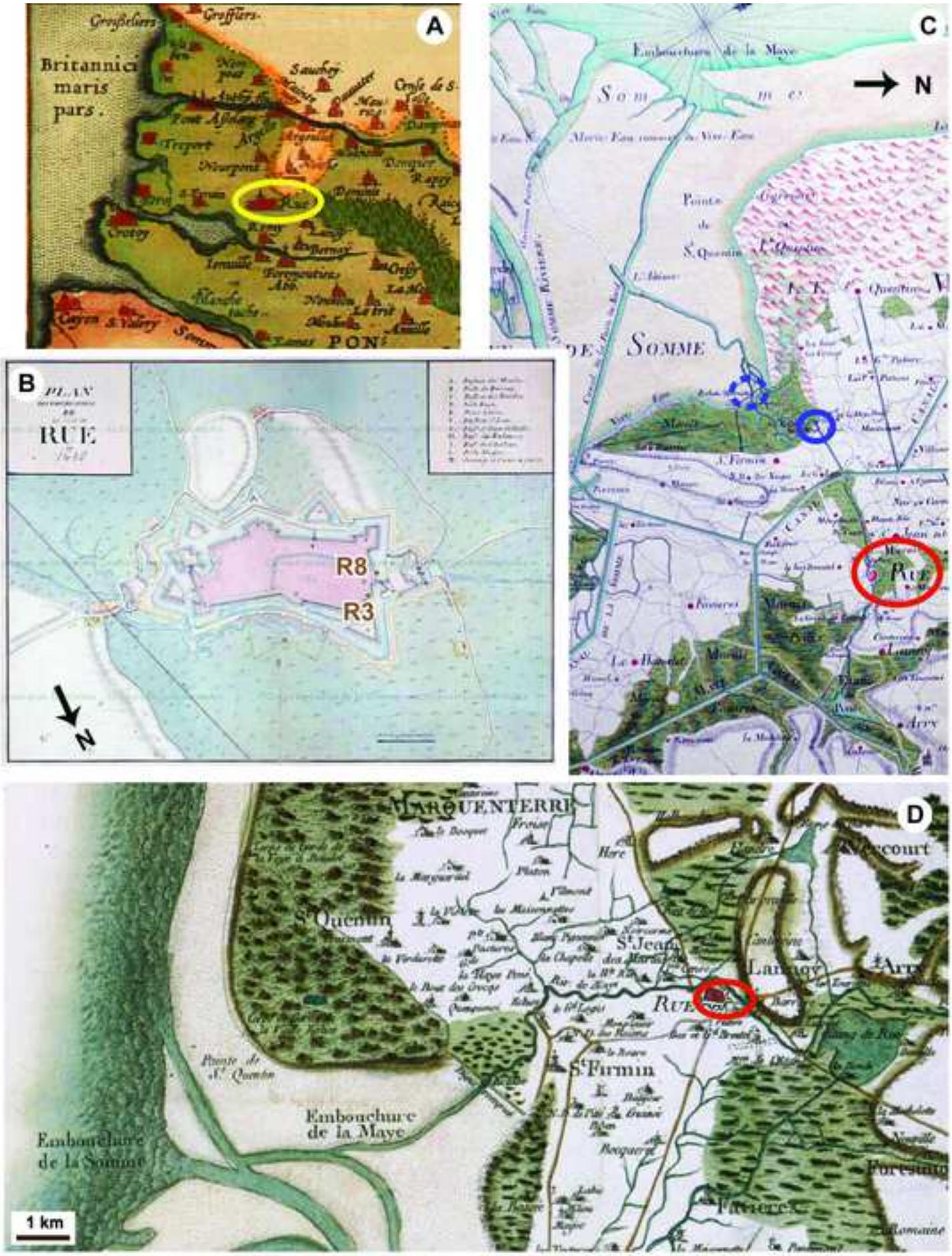

Figure

Click here to access/download;Figure;Fig11.jpg

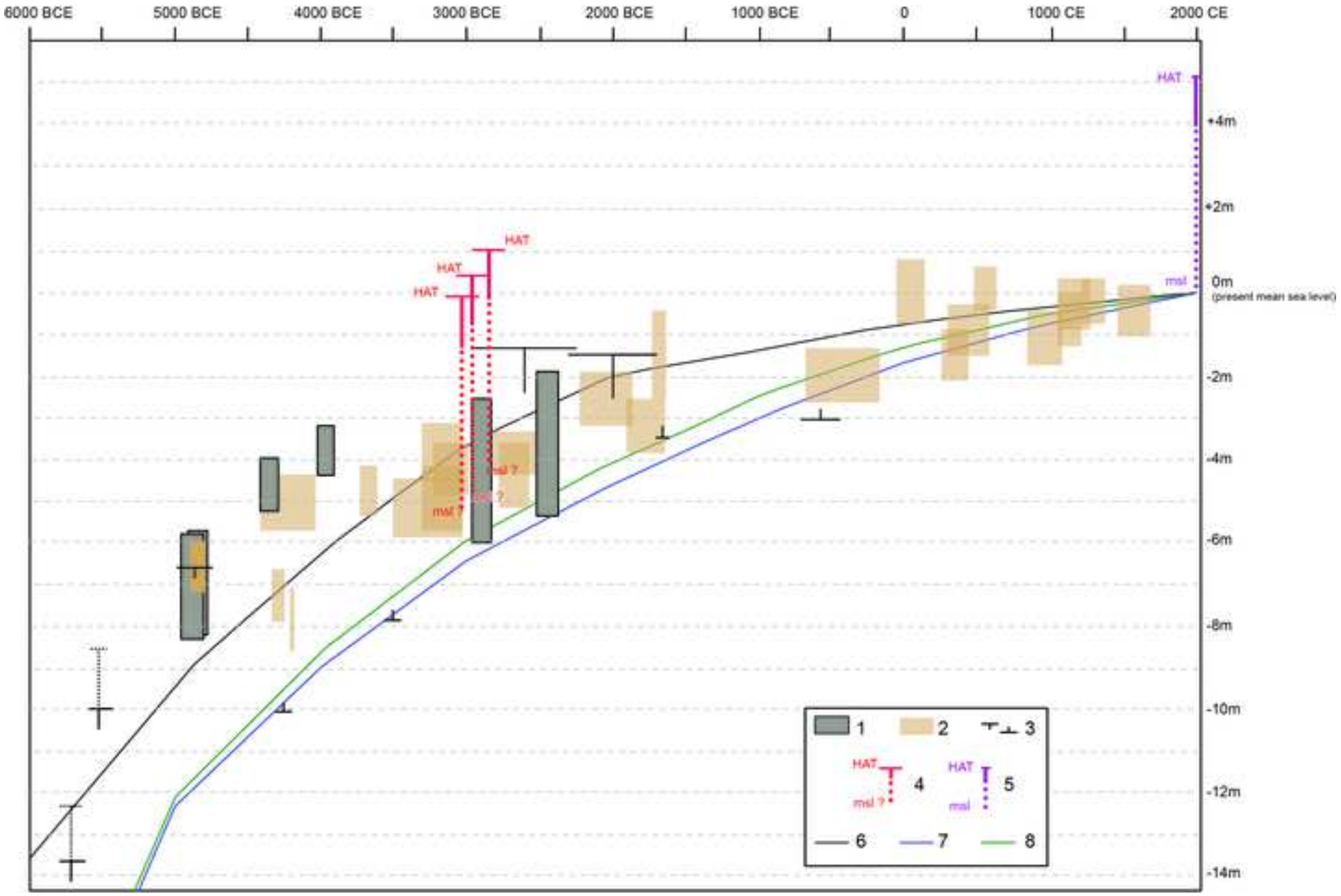

Figure

Click here to access/download;Figure;fig12.jpg

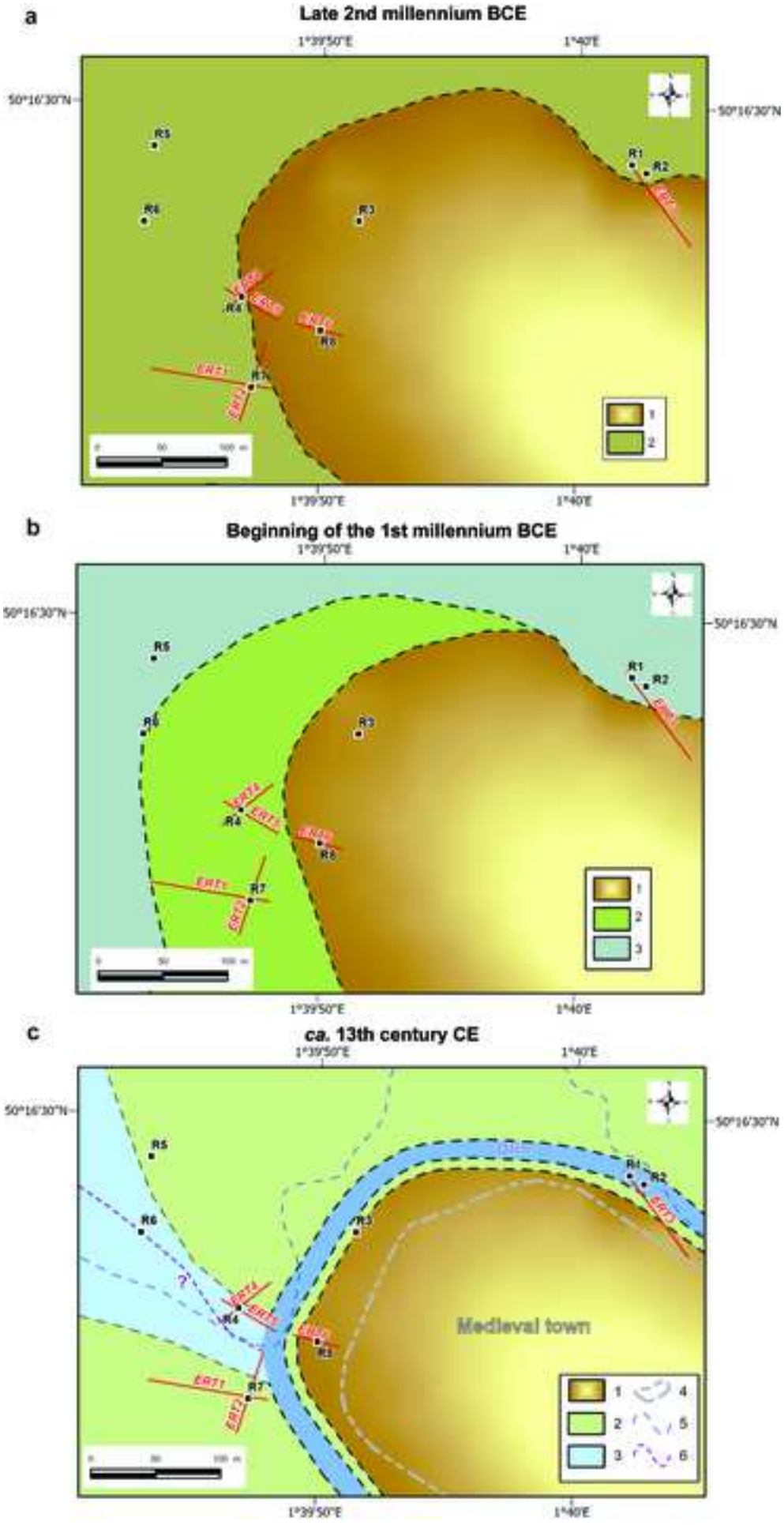

Table

Profile reference	starting point (EPSG 2154)		ending point (EPSG 2154)		lenght (m)
ERT1	50°16'23"N	1°39'43"E	50°16'23"N	1°39'48"E	96
ERT2	50°16'24"N	1°39'48"E	50°16'22"N	1°39'47"E	64
ERT3	50°16'31"N	1°40'E	50°16'27"N	1°40'40"E	160
ERT4	50°16'25"N	1°39'46"E	50°16'26"N	1°39'48"E	51.2
ERT5	50°16'25"N	1°39'46"E	50°16'25"N	1°39'48"E	51.2
ERT6	50°16'24"N	1°39'49"E	50°16'24"N	1°39'51"E	38.4
ERT7	50°16'54"N	1°40'51"E	50°16'53"N	1°40'56"E	96
ERT8	50°5'28"N	1°25'39"E	50°05'26"N	1°25'36"E	64

Table

Laboratory number	Core	Depth	Material	Conventional radiocarbon age	Calibrated date (2σ)
Poz-54987	R4	144 cm	Charcoal	900±30 BP	1039-1210 CE
Poz-54988	R4	167 cm	Charcoal	990±30 BP	989-1052 CE
Poz-54989	R4	380 cm	Peat	2980±30 BP	1297-1111 BCE
Poz-54991	R4	418 cm	Peat	4285±30 BP	2934-2875 BCE
Poz-54992	R4	446 cm	Wood	4690±40 BP	3532-3368 BCE
Poz-54993	R4	477 cm	Charcoal	5200±35 BP	4057-3953 BCE
Poz-54995	R5	122 cm	Peat	1625±30 BP	380-536 CE
Poz-54997	R5	367 cm	Peat	3235±35 BP	1565-1434 BCE
Poz-54998	R5	460 cm	Peat	4960±35 BP	3798-3654 BCE
Poz-54999	R5	504 cm	Wood	5000±40 BP	3824-3695 BCE
Poz-55001	R6	179 cm	Plant	880±30 BP	1117-1221 CE
Poz-55003	R6	408 cm	Peat	2600±35 BP	834-752 BCE
Poz-55004	R6	490 cm	Peat	5000±40 BP	3824-3695 BCE
Poz-55005	R7	260 cm	Peat	2900±30 BP	1134-1004 BCE
Poz-55006	R7	310 cm	Peat	4410±35 BP	3113-2915 BCE
Poz-55007	R7	365 cm	Peat	4745±35 BP	3637-3500 BCE